RAPHAEL POUSA DOS SANTOS

RAINFALL VARIABILITY AND AVAILABILITY OF WATER RESOURCES IN THE LAST 40 YEARS IN WESTERN BAHIA, BRAZIL

Thesis submitted to the Applied Meteorology Graduate Program of the Universidade Federal de Viçosa in partial fulfillment of the requirements for the degree of *Doctor Scientiae*.

Adviser: Marcos Heil Costa

VIÇOSA – MINAS GERAIS
2022

Ficha catalográfica elaborada pela Biblioteca Central da Universidade Federal de Viçosa - Campus Viçosa

T
S237r
2022

Santos, Raphael Pousa dos, 1982-
Rainfall variability and availability of water resources in the last 40 years in western Bahia, Brazil / Raphael Pousa dos Santos. – Viçosa, MG, 2022.
1 tese eletrônica (79 f.): il. (algumas color.).

Orientador: Marcos Heil Costa.
Tese (doutorado) - Universidade Federal de Viçosa, Departamento de Engenharia Agrícola, 2022.
Referências bibliográficas: f. 74-79.
DOI: https://doi.org/10.47328/ufvbbt.2022.257
Modo de acesso: World Wide Web.

1. Hidrometeorologia - Bahia - Análise. 2. Mudanças climáticas. 3. Segurança hídrica. I. Costa, Marcos Heil, 1965-. II. Universidade Federal de Viçosa. Departamento de Engenharia Agrícola. Programa de Pós-Graduação em Meteorologia Aplicada. III. Título.

CDD 22. ed. 551.57098142

Bibliotecário(a) responsável: Alice Regina Pinto CRB6 2523

RAPHAEL POUSA DOS SANTOS

RAINFALL VARIABILITY AND AVAILABILITY OF WATER RESOURCES IN THE LAST 40 YEARS IN WESTERN BAHIA, BRAZIL

Thesis submitted to the Applied Meteorology Graduate Program of the Universidade Federal de Viçosa in partial fulfillment of the requirements for the degree of *Doctor Scientiae*.

APPROVED: March 03, 2022

Assent:

Raphael Pousa dos Santos
Author

Marcos Heil Costa
Adviser

Para minha mãe, meu irmão, e meus avós.

ACKNOWLEDGMENTS

Quero agradecer à minha mãe, que mesmo de longe, passando por todos os percalços que a vida lhe impôs nesse período se mostrou firme e forte, sempre me apoiando, sempre me mandando uma mensagem, mesmo que não estivesse tudo bem, mas estava tudo bem. Ao meu irmão, que está a alguns km de distância de mim e eu só o vejo algumas vezes no ano, mas está sempre comigo. À minha avó que está sempre me abençoando. E ao meu avô, que talvez dele, eu puxei toda a serenidade de encarar essa vida. E que privilégio eu poder agradecer a eles em vida.

As três importantes pessoas que me acompanharam até um tempo nesse período e não estão mais aqui comigo. Aos meus tios e padrinhos Maria Inês e Ennio, que sempre demonstram orgulho das minhas conquistas, e que tenho certeza que ainda estão aqui comigo. E ao Yoshio, meu padrasto, que sempre esteve me apoiando.

À tia Maria e ao tio Doni que sempre fizeram questão de me ver quando eu voltava para Cachoeira.

A todos meus amigos:

Ao Gabriel, Aninha, Victor e Carol, por toda a cumplicidade, discussões, ideias e companheirismo, que mesmo quando essa etapa foi pesada, com vocês encontrei leveza e empatia.

À Pauline, Vitor Fontes, Pimenta, Luiz, Livinha, Matheus, Vinicius, Marina, Flavia, Verônica, Argemiro, vocês são peças que se somaram nesse caminho.

À Emily, Livia, Gabrielle e Fabi, vocês são inspiração de persistência e por acreditar em uma educação (e trabalho) que pode fazer diferença nesse mundo.

Aos amigos da MICROMET, Gabriel, Bruna, Gisele e Claudinho, obrigado pelo apoio.

Ao Carlos, Noele e Rafael, obrigado pelas cervejas divididas e muitas discussões.

À Lea e Larissa pela companhia durante a pandemia e que fizeram com que esse tempo fosse mais ameno e impactou em todo esse trabalho.

Aos amigos do INPE, onde nos tempos em que estive lá, talvez eu não tenha percebido a ciência por trás de todo o meu trabalho com vocês, mas durante todo esse período de agora, me vinha à mente muitos dos momentos desse trabalho e do como as peças se encaixavam.

Aos amigos espalhados por esse mundo: Cachoeira Paulista, Lorena, Rio de Janeiro, Dubai, São Paulo, São José dos Campos, Chapecó, Rio Grande do Sul, e Caraguatatuba, vocês estão comigo desde sempre, obrigado por toda amizade nesses anos, por todas as videochamadas e mensagens que fizeram diminuir a distância no mapa.

Aos professores que ajudaram a construir, peça por peça, o caminho dessa tese. Parece que em um corte cinematográfico, eu vasculhei desde lá do fundo da memória os primeiros professores e chegar até aqui é um apanhado dessas peças para formar um quebra-cabeça. Sem essa profissão, o mundo não andaria.

Ao professor Marcos, por ser inspiração a todos que o rodeiam. Pela maestria que conduz a ciência e o ensino. Por toda a paciência e exigência que tem/faz com todos, fazendo cada um esmiuçar os entreves de uma pesquisa e nos faz enxergar cada detalhe não visto.

À Graça Freitas, pela competência e acolhimento que tem com todos os alunos. Uma pessoa fundamental para o programa de Meteorologia Aplicada.

À Universidade Federal de Viçosa, pela oportunidade de realizar a pós-graduação.

O presente trabalho foi realizado com apoio da Coordenação de Aperfeiçoamento de Pessoal de Nível Superior – Brasil (CAPES) – Código de Financiamento 001.

À Coordenação de Aperfeiçoamento de Pessoal de Nível Superior (CAPES), pela concessão da bolsa de estudos.

Essa caminhada é conjunta, mas também é de coração.

Obrigado.

Rios sem discurso

Quando um rio corta, corta-se de vez.
o discurso-rio de água que ele fazia;
cortado, a água se quebra em pedaços,
em poços de água, em água paralitica.
Em situação de poço, a água equivale
a uma palavra em situação dicionária:
isolada, estanque no poço dela mesma,
e, porque assim estanque, estancada;
e mais: porque assim estancada, muda,
e muda porque com nenhuma comunica,
porque cortou-se a sintaxe desse rio,
o fio de água por que ele discorria.

o curso de um rio, seu discurso-rio,
chega raramente a se reatar de vez;
um rio precisa de muito fio de água
para refazer o fio antigo que o fez.
salvo a grandiloquência de uma cheia
lhe impondo interina outra linguagem,
um rio precisa de muita água em fios
para que todos os poços se enfrasem:
se reatando, de um para outro poço,
em frases curtas, então frase e frase,
até a sentença-rio do discurso único
em que se tem voz a seca ele combate.

João Cabral de Melo Neto.

ABSTRACT

SANTOS, Raphael Pousa dos, D.Sc., Universidade Federal de Viçosa, March, 2022. **Rainfall variability and availability of water resources in the last 40 years in Western Bahia, Brazil**. Adviser: Marcos Heil Costa.

In recent decades, the increased demand for food, both nationally and internationally has driven agricultural expansion in Brazil. Biophysical, social, and economic factors have made Brazilian Cerrado one of the biomes with the greatest capacity to occupy its territory with crops. This expansion has started in the 1970s, and currently, the Brazilian Cerrado accounts for 40% of the national agricultural production. Western Bahia is one of the most active agricultural frontiers globally in this biome, with a rapid increase in agricultural and irrigated areas. This study aims to make a hydrological, climatic, and water availability analysis and the impacts that this growth can caused in the last 40 years, from 1980 to 2020. First, considering the period 1980-2015, a climate analysis showed a significant reduction in rainfall of up to 12% since the 1980s, and a reduction in river flows, both for dry and rainy seasons. Seven sub-regions in Western Bahia were identified with a potential risk of conflicts over water use. These regions experienced a 150-fold increase in the irrigated area since 1990s and 90% from 2010 to 2018. In recent years, these conflicts have become more frequent due to a combination of factors: climate variability, increased demand for water resources, and continued trends of decreasing precipitation. Second, in a complementary analysis, extending the analysis period to 2020, it was investigated how the interaction of large-scale (represented by Atlantic Multidecadal Oscillation – AMO) and mesoscale (topography) processes can affect the region's climate variability. Precipitation and river discharge data indicate a continued reduction. Precipitation has decreased by 11.5% since 1980s. The rainiest bimester, December and January (DJ), indicated a significant negative correlation with AMO ($R = -0.62$, $\alpha = 0.01$), showing that precipitation decreases in DJ when the AMO index is positive. Within these 40 years, the five rainiest and driest DJs were selected. The rainiest ones showed that large-scale mechanisms interact with the local topography, promoting a stronger convection and high rainfall rates over the region. There is a regional suppression of convection for this driest DJ bimesters, including over the topographic gradient, shifting the convection center further west, and decreasing rainfall in Western Bahia. The climate variability in the region and the intense growth of irrigation have made the potential of conflicts over water use more frequent. Furthermore, with the continuous increase in North Atlantic temperatures, it is unlikely that the wet climatic conditions existing before the early 1990s will return. Thus, precipitation in the region will be

affected, putting pressure on water availability and directly impacting economic activities dependent on climate.

Keywords: Climate change. Water security. Hydroclimatic analysis.

RESUMO

SANTOS, Raphael Pousa dos, D.Sc., Universidade Federal de Viçosa, março de 2022. **Variabilidade das chuvas e disponibilidade dos recursos hídricos nos últimos 40 anos no Oeste da Bahia, Brasil**. Orientador: Marcos Heil Costa.

Nas últimas décadas, o aumento da demanda por alimentos tanto nacional quanto internacionalmente impulsionou a expansão agrícola no Brasil. Fatores biofísicos, sociais e econômicos fizeram do Cerrado brasileiro um dos biomas com maior capacidade de ocupação de seu território com cultivos agrícolas. Essa expansão teve início na década de 1970 e, atualmente, o Cerrado brasileiro responde por 40% da produção agrícola nacional. O Oeste da Bahia é uma das fronteiras agrícolas mais ativas do mundo neste bioma, com rápido aumento de áreas agrícolas e irrigadas. Este estudo tem como objetivo fazer uma análise hidrológica, climática, de disponibilidade hídrica e dos impactos que esse crescimento causou nos últimos 40 anos, de 1980 a 2020. Primeiramente, considerando o período 1980-2015, uma análise climática mostrou uma redução significativa nas chuvas de até 12% desde a década de 1980 e redução das vazões dos rios, tanto na estação seca quanto na chuvosa. Sete sub-regiões do Oeste da Bahia foram identificadas com risco potencial de conflitos pelo uso da água. Essas regiões tiveram um aumento de 150 vezes na área irrigada desde 1990 e 90% de 2010 a 2018. Nos últimos anos, esses conflitos se tornaram mais frequentes devido a uma combinação de fatores: variabilidade climática, aumento da demanda por recursos hídricos e continuidade das tendências de diminuição da precipitação. Em segundo lugar, em uma análise complementar, considerando o período 1980-2020, investigou-se como a interação de processos de grande escala (representada pela Oscilação Multidecadal do Atlântico – AMO) e de mesoescala (topografia) podem afetar a variabilidade climática da região. Os dados de precipitação e descarga fluvial indicam uma redução contínua. A precipitação diminuiu 11,5% desde a década de 1980. O bimestre mais chuvoso, dezembro e janeiro (DJ), indicou uma correlação negativa significativa com a AMO ($R = -0,62$, $\alpha = 0,01$), mostrando que a precipitação diminuiu em DJ quando o índice AMO é positivo. Nesses 40 anos, foram selecionados os cinco DJs mais chuvosos e secos. Os mais chuvosos mostraram que mecanismos de grande escala interagem com a topografia local, promovendo convecção mais forte e altas taxas de chuva sobre a região. Há uma supressão regional da convecção para os bimestres DJ mais secos, inclusive sobre o gradiente topográfico, deslocando o centro de convecção mais para oeste e diminuindo as chuvas no Oeste da Bahia. A variabilidade climática da região e o intenso crescimento da irrigação tornaram mais frequente o potencial de conflitos pelo uso da água. Além disso, com

o aumento contínuo das temperaturas do Atlântico Norte, é improvável que as condições climáticas úmidas existentes antes do início da década de 1990 retornem. Assim, a precipitação na região será afetada, pressionando a disponibilidade hídrica e impactando diretamente as atividades econômicas dependentes do clima.

Palavras-chave: Mudanças climáticas. Segurança hídrica. Análises hidroclimáticas.

LIST OF FIGURES

CHAPTER 1

CHAPTER 2

SUMMARY

General Introduction

The Brazilian Cerrado is the second largest biome in the country, with approximately 204 million hectares, representing 24% of the national territory. This biome is considered the richest tropical savanna globally in terms of biodiversity, and eight of the twelve Brazilian river basins are present in the biome (EMBRAPA, 2020). In addition, it is one of the regions with the highest growth in agriculture in recent decades, with agricultural production corresponding to 40% of the national total (EMBRAPA, 2020).

This Brazilian biome enters the projections of several studies to become one of the main food suppliers in the world (Soterroni et al., 2019). This role is related to the expansion of agricultural in Brazil's central, northeastern and northern regions from the late 1970s (Dias et al., 2016). At that time, the Cerrado was not considered a potential biome for agricultural use due to its nutrient-poor soil and considerable acidity rates, which making it an unproductive land (Faleiro et al., 2008; Dionizio et al., 2020). However, in the late 1970s, with the depletion of agricultural land further south, the Brazilian government created agricultural financing programs to develop the midwest region of the country, such as *Programa de Desenvolvimento da Região Centro-Oeste* (*Polocentro*) (EMBRAPA, 2020). These programs subsidize technologies for soil improvement, improving soil management techniques, such as liming (correction of soil acidity by applying lime) and soil fertilization with the application of phosphate and potassium (Dionizio et al., 2020). After developing in the central-western region, agricultural areas expanded further into the Cerrado of northeastern Brazil, with predominantly sandy soils and greater climate variability (Araujo et al., 2019).

Thus, the newest and last agricultural frontier in the country is the MATOPIBA (acronym formed by the states of Maranhão, Tocantins, Piuaí, and Bahia). The main aspects that led to the emergence of this region are: the high extension of areas with flat relief, which facilitates intensive crop mechanization; the presence of soils with physical properties that favor this mechanization; low cost of land for production, compared to the other areas of the Cerrado; and proximity to the port of Itaqui in São Luis, Maranhão (EMBRAPA, 2020). Another attraction supporting the rise of crops in this region was the mean climatic conditions, mainly the precipitation, which annual mean between 1000 and 1500 mm, providing favorable conditions for agricultural expansion (Pimenta et al., 2021).

Particularly, the most productive region of the states is localized in Bahia, an area known as Western Bahia that concentrates 50% of all grain produced in MATOPIBA (Dionízio et al., 2020). The expansion of agriculture in this region started in the 1980s with the cultivation of

soybeans. With technological development, it was possible to cultivate other crops in the region such as cotton, corn, beans, and coffee (AIBA, 2020). Western Bahia has 10 Mha and in 2020, croplands covered approximately 3 Mha, of which 218,000 ha were irrigated (Pimenta et al., 2021). The region is a reference in large-scale production in the sector, representing 35% of the agricultural GPD (Gross Domestic Product) in the state of Bahia.

Western Bahia has a topography that facilitated the development of agriculture allied to an abundance of natural resources, especially water availability. The region includes three river basins (Rio Grande, Rio Corrente, and the northern part of Rio Carinhanha). It has undergone intense irrigation growth in the last decades (Pimenta et al., 2021). Irrigation is an important practice that increases productivity and the growing season in the region where precipitation does not support the crop water demand.

Irrigation efficiency depends mainly on irrigation management, directly impacting productivity, water availability and quality (ANA, 2017). The technology that accompanies irrigation - such as supplies, machinery, and services - tends to improve the environmental quality of the regions where they are installed, adopting better management techniques, such as no-till farming and better use of the soil (ANA, 2017). One of the managements necessary for irrigation efficiency is based on the values of crop evapotranspiration or the depth needed for irrigation. The water use efficiency of plants depends on the amount of water each crop needs at each stage of development. With well-efficient irrigation, productive efficiency is expected (ANA, 2017).

The extensification of irrigated areas has grown in the last 35 years, but the total percentage of irrigated areas in Western Bahia is still considered small, just under 8% (ABAPA, 2020). The growth in recent years has also made the region advance socioeconomically, and the irrigated area contributes 34% of the Gross Value of Agricultural Production (ABAPA, 2020). The projection of irrigated area for 2030 indicate an increase in irrigated area by > 30,000 ha in the entire Rio Grande basin. In the Corrente Basin, it will increase between 10,000 and 30,000 ha (ANA, 2017).

Irrigated agriculture can find difficult in dry years. Although the region has a well-defined rainy season, a hydrological drought can affect a region. In 2015, Western Bahia had annual precipitation of 674 mm (Pousa et al., 2019) and a delay in the onset of the rainy season that only started in January 2016 (AIBA, 2016). Due to these facts, soybean yields had a 40% reduction in the 2015/2016 harvest compared to the previous season, while corn had a 38.6%

reduction in the same period. Climate variability was not the only cause of yield reduction in this specific year, as high supply costs should also be considered (AIBA, 2016).

This thesis investigates the considerable increase of irrigated areas in Western Bahia and the climate variability in the region in the last 40 years. Chapter 1 presents a hydroclimatic analysis of water resources for the 1980-2015 period. I used a long-term time series of precipitation and river discharge to explore the availability of water resources for irrigation. I analyzed the considerable irrigation growth since the 2000s and, consequently, water use conflicts in some basins of Western Bahia. I mapped seven regions where growing water use combines with climate variability, reducing water availability, and increasing demand for water resources. In Chapter 2, I extended the long-term series of river discharge and updated the precipitation database (with a finer resolution) for the period 1981-2020. To analyze the climate variability in the region, I investigate how large-scale processes (Atlantic Multidecadal Oscillation – AMO) and mesoscale processes (orographic) are related to the precipitation patterns in the region.

CHAPTER 1. CLIMATE CHANGE AND INTENSE IRRIGATION GROWTH IN WESTERN BAHIA, BRAZIL: THE URGENT NEED FOR HYDROCLIMATIC MONITORING

Pousa, R., Costa, M.H., Pimenta, F.M., Fontes, V.C., Castro, M., 2019. **Climate change and intense irrigation growth in Western Bahia, Brazil: The urgent need for hydroclimatic monitoring**. Water (Switzerland) 11. https://doi.org/10.3390/w11050933

1.1. Introduction

The relationship between water and conflict is an area of continued interest and debate in both the policy and water resources literature and in the popular press (Yoffe et al., 2004). Conflicts arise by several socioeconomic, political, or biophysical causes, including proximity to the water source, government type, aridity, climate variability and change, and rapid population growth. The dispute becomes much more challenging when there are multiple causes for the conflict. This work provides a case study of a region where two factors, climate change and intense irrigation growth, contribute to increased friction on the use of water resources: Western Bahia, in Brazil.

The western part of the state of Bahia is one of the most active agricultural frontiers of the world, where land use transition started in 1985 (Batistela et al., 2009). Western Bahia (Figure 1.1) is part of a wider region called MATOPIBA (acronym formed by the states of Maranhão, Tocantins, Piauí, and Bahia), an agricultural frontier in the Cerrado biome in Brazil, and characterized by rapid changes in land cover and land use for cropland, especially soybean, and agricultural intensification through the adoption of new technologies, leading to high yields. In Western Bahia, cropland area has reached 2 million hectares in the 2016/2017 growing season, mainly soybeans, cotton, and maize (AIBA, 2018).

A major difference between Western Bahia and the rest of MATOPIBA is that the impressive extensification has been followed by a no less impressive increase in irrigated area, which grew from 9 pivots in 1985 to 1550 center pivots in 2016 (ANA, 2017). The region includes three river basins (Rio Grande, Rio Corrente, and the northern part of the Rio Carinhanha), all tributaries of the São Francisco River, and also sits on the top of the Urucuia aquifer (ANA, 2013), a vast geological formation that is connected to the rivers, and helps regulate their seasonality and interannual variability. Five small hydroelectric plants operate in the region, all on tributaries of the Rio Grande upstream of the town of Barreiras (Figure 1.1), with power ranging from 450 kW to 25 MW (WMEPE, 2019).

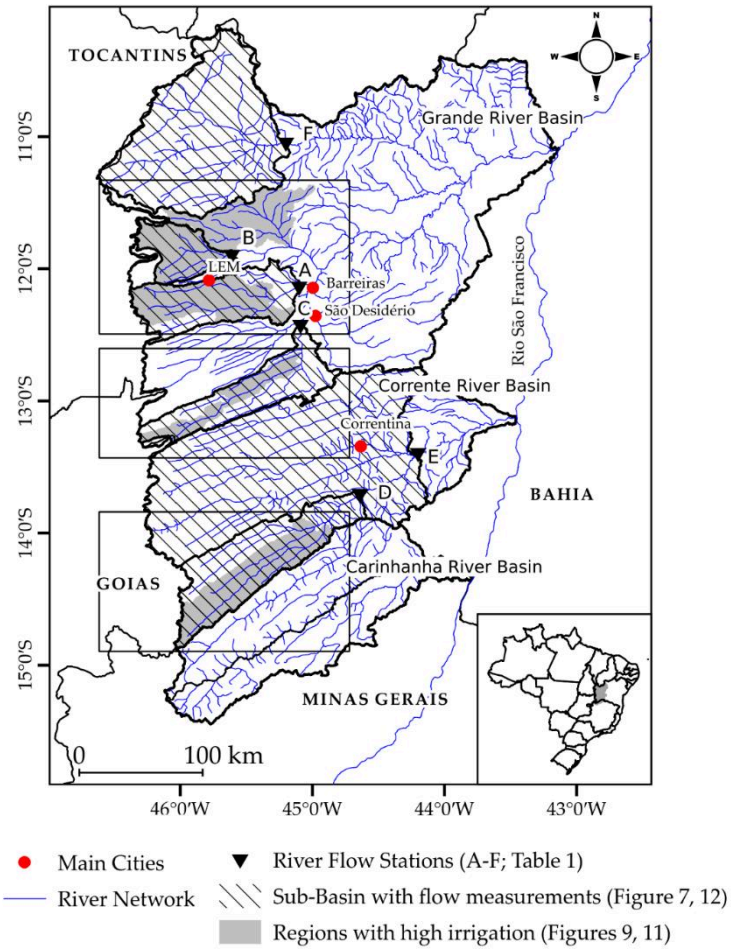

Figure 1. 1. Study area representing the river networks, sub-basins with flow measurements analyzed in this study (hatched areas), regions with high irrigation (gray areas), and the location of main towns. LEM is the town of Luis Eduardo Magalhães. The rectangles represent the zoom areas detailed in Figure 1.5. River flow stations A–F are described in Table 1.1.

The long-term (1980–2015) precipitation, evapotranspiration, and runoff for the region are 1060 mm year^{-1}, 860 mm year^{-1}, and 200 mm year^{-1}, respectively. However, the region is located in the transition between the seasonally dry Cerrado biome to the west (annual precipitation >1200 mm year^{-1} and a six-month rainy season, from mid-October to mid-April) and the semi-arid Caatinga biome to the east (annual precipitation <800 mm year^{-1} and a four-month rainy season). Precipitation, evapotranspiration, and runoff are seasonal. Precipitation typically varies from 0–10 mm month^{-1} in the driest months (June, July, August) to about 150–200 mm month^{-1} in the rainiest months (December and January). Monthly evapotranspiration (from MODIS MOD16 product) typically varies between 20 mm month^{-1} in September and 85 mm month^{-1} in February. Despite the high seasonality in precipitation, the seasonal variability in runoff is relatively small, with maximum discharge about three times greater than the

minimum discharge, which is an indication of the strong regulation provided by the Urucuia aquifer. Temperatures and solar radiation are high around the year and, with the aid of irrigation, would allow for year-round crops (five to six crop growing seasons in two years), limited only by phytosanitary regulations. These circumstances have contributed to the intense growth of irrigation in the region (MDIC, 2018).

Conflicts over the use of water have become common in the region in the last decade, however few of them have been documented. Maybe the first documented conflict happened in 2010. The hydropower station *Sítio Grande* on the Rio das Fêmeas, a tributary of the Rio Grande, is the largest plant in the region and has a water permit of 12 $m^3 s^{-1}$, the largest water permit in the region, about 1/3 of the water rights granted in the Rio Grande basin (Almeida et al., 2014). Despite being the largest grant, this is a non-consumptive use of water, as the water is not withdrawn from the river, but instead it must be available at the river to flow through the turbines. The conflict happened during the initial filling of the lake, which interrupted the flow of the river for several days with environmental and social consequences.

Conflicts kept being reported informally through social networks, personal communications, etc. Another formal documentation happened in 2015, an El Niño year when the region experienced a severe drought (2015 annual rainfall was 674 mm, one of the lowest on record). On 11 December 2015, the Rio Corrente Basin Committee requested a temporary suspension on the concession of water use permits on the basin until further criteria for water permits on the basin are defined (CBHRC, 2019). On 2 November 2017, the usually peaceful town of Correntina (pop. population 32,000) made the national headlines (G1, 2017), when about 500 people invaded one farm that received recent irrigation systems and destroyed a significant part of their facilities and equipment as a way of protesting against the appropriation of water by agribusiness. A week after, on 11 November, approximately 10,000 people marched peacefully through Correntina, in defense of the Rio Corrente and its tributaries (Correio 24 horas, 2017).

Although the water use conflicts in the region are usually attributed to the immense growth rate of irrigation systems, climate variability may also play an important role. Being in the transition between the semi-arid and the seasonally dry tropical climate regions, Western Bahia may be a serious candidate for climate change. This study makes an hydroclimatic analysis of the water resources in Western Bahia, from both the supply and demand viewpoints.

1.2. Data and methods

Data and methods used in this analysis are summarized in Figure 1.2. Long-term time series of precipitation and river discharge are analyzed to evaluate the availability of water resources for irrigation, while maps of irrigation areas and interviews with irrigators are produced to evaluate the demand of water resources. We conclude with recommendations to improve water management and avoid further water conflicts.

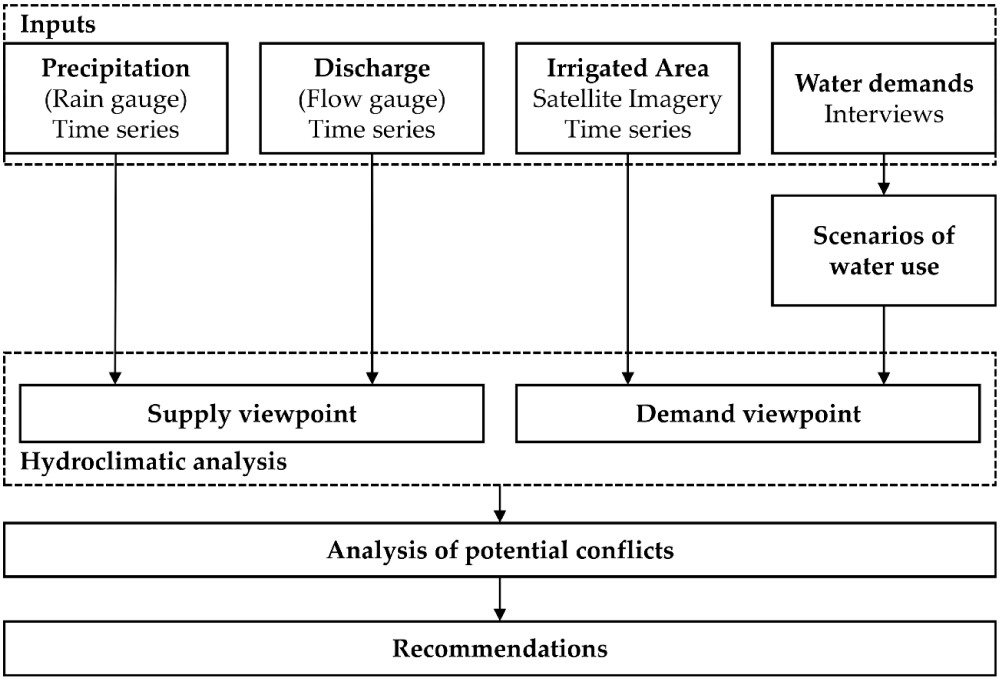

Figure 1. 2. Flowchart illustrating the data and methods.

1.2.1. Precipitation and River Flow

Precipitation data in the region have been available through the INMET (*Instituto Nacional de Meteorologia*) and ANA (*Agência Nacional das Águas*) weather station and rain gauge networks since the 1930s, but the network was sparse and the time series were frequently interrupted. A somewhat dense network was available only in the late 1970s. To characterize regional patterns, the daily precipitation dataset of Xavier et al. (2015) was used, which is available at a grid resolution of 0.25 × 0.25 (approximately 28 km × 28 km) for a 36-year period of 1980–2015. This dataset was assembled from the available rain gauge, conventional, and automatic weather stations. Original data were quality-controlled, and six different interpolation methods were tested (average of the five nearest data points; natural neighbor; thin plate spline; inverse distance weighting; angular distance weighting; and ordinary point

kriging). The accuracy of the interpolation methods was evaluated by a cross-validation procedure, in which an observed data point was temporarily removed from the database, and then used to test the estimated value by each interpolation method at the location of the station. Angular distance weighting was considered the method with best skill (Xavier et al., 2015). To evaluate longer trends (before 1980), the station of Barreiras (WMO code 83236) was also used, which has nearly continuous data since 1961.

The daily river flow data (m^3/s) used are provided by ANA. The fluviometric data are available since the 1930s, with a low density of stations and significant gaps. From 1930s to 1970s, there are about 30% of gaps in the data series and some discontinued stations. Quantity and quality of data increased in the 1970s, with only 2% of gaps, and we initially selected 25 river flow stations with few gaps since 1978.

The granting of water use permits in the Grande and Corrente basins is an attribution of the State of Bahia, which uses the criterion that 80% of Q_{90} can be granted for human use (according to State Decree number 6296 of 21 March 1997). Q_{90} is the flow expected to be present in the river during at least 90% of the time, i.e., during 90% of the time series used in the calculation, there is a flow equal or greater than Q_{90} in the river.

To follow this criterion, our analyses of water availability are based on the flow duration curve of specific sections of the rivers. A flow duration curve is a cumulative frequency curve that shows the percent of time specified discharges were equaled or exceeded during a given period. Here, Q_{90} was calculated using the long-term series (LT Q_{90}), which is a more common criterion for granting water use permits, but we also calculate Q_{90} using two periods, to characterize hydroclimate change.

Although we analyzed data for 25 fluviometric stations, six stations were selected for a deeper analysis (Table 1.1, Figure 1.1). These stations are spread throughout the region and are representative of the regional variability. Moreover, four stations were chosen because they have dense irrigation systems upstream (A–D), while two of them (E,F) were chosen for their low irrigation density upstream.

The flow stations drain relatively large areas, and (with the exception of station B) may not be representative of the densest irrigated areas. Thus, seven ottobasins with the highest concentration of center pivots (represented by gray areas in Figure 1.1) were also analyzed. Ottobasins, or Otto-codified hydrographic basins, are areas of contribution of the stretches of the hydrographic network coded according to the topological system proposed by Otto Pfafstetter (Pfafstter, 1989; Verdin et al., 1999) and officially adopted by ANA to uniquely

identify contribution areas in any watershed using a simple 10-base code. The system is hierarchical and recursive, and the higher number of digits in the ottobasin code implies a higher level of sub-division of a watershed.

Table 1. 1. Selected river flow stations. The letters correspond to the labels of stations in Figure 1.1**.**

	ANA Station Code	River	Station Name	Municipality	Drainage Area (km^2)	Station Coordinates
A	46543000	Rio de Ondas	Fazenda Redenção	Barreiras	5383.758	12°08'S, 45°06'W
B	46570000	Rio de Janeiro	Ponte Serafim	Barreiras	2522.118	11°54'S, 45°36'W
C	46415000	Rio Grande	Sítio Grande	São Desidério	4943.866	12°25'S, 45°05'W
D	45840000	Rio Formoso	Gatos	Jaborandi	7132.696	13°42'S, 44°38'W
E	45910001	Rio Corrente	Santa Maria da Vitória	Santana	29,643.660	13°24'S, 44°12'W
F	46790000	Rio Preto	Formosa do Rio Preto	Formosa do Rio Preto	14,326.870	11°03'S, 45°12'W

1.2.2. Statistical Tests

We applied four statistical analyses to detect changes in the rainfall time series. First, we applied the non-parametric Pettitt´s test (Pettit, 1979) for detecting changing points to the region-wide precipitation time series. This is a rank-based and distribution-free test for detecting a significant change in the mean of a time series and it is particularly useful when no hypothesis is required about the location of the changing point. The Pettitt test has been widely applied to detect changes in the observed hydroclimatic time series (Verstraeten et al.,2006; Rybski et al., 2006), and can only be applied to continuous time series. Considering a sequence of random variables $X_1, X_2, \ldots, X_T$, which have a change point at $t = \tau$. As a result, ($X_1, X_2, ..., X_\tau$) have a common distribution function $F_1(X)$, but ($X_{\tau+1}, X_{\tau+2}, ..., X_T$) are distributed as $F_2(X)$, where $F_1(X) \neq F_2(X)$. The null hypothesis H_0 for this test is that the observations are independent and identically distributed (no change, or $\tau = T$), and is tested against the alternative hypothesis H_1: change (or $1 \leq \tau < T$); using the non-parametric statistic $K_T = \max|U_{t,T}|$ where:

$$U_{t,T} = \sum_{i=1}^{t} \sum_{j=t+1}^{T} sign(X_t - X_j).$$

The confidence level for a change-point is defined as

$$\rho = exp\left(\frac{-6\,K_T^2}{T^3 + T^2}\right).$$

Second, we applied a classical Student´s t-test to test the null hypothesis that the annual mean precipitation is not significantly different from one period to the other, where periods are divided at $t = \tau$, obtained by the Pettitt´s test.

Third, we applied the Mann–Kendall test for trends in the time series, a non-parametric, distribution-free test that makes no assumptions of linearity or distribution of the values. This test has been recommended widely by the World Meteorological Organization for general trend analysis of time series (Mitchell et al., 1966). Finally, we used box plots to evaluate the interannual variability of precipitation.

1.2.3. Irrigated Area

The irrigated area by center pivots was obtained by a four-step procedure. First, imagery from Landsat 5, 7, and 8 for the period 1990 to 2018 was processed using the Google Earth Engine cloud. The images were filtered using the median of the pixels for the dry period (April to September) and mosaicked for the study region, to produce a single region mosaic per year. Second, the filtered map was merged with the center pivots data from Landau et al. (2014) and from the OpenStreetMaps project to obtain an initial pivots map of the region. Then, duplicated features and topology errors were removed from the dataset. Third, with the aid of the visible bands (RGB) and the normalized difference vegetation index (NDVI) from the generated mosaics, the center pivot features were digitized or erased according to the recognition in the images of each year. Finally, the annual center pivot geometries went through a trend and precision analysis of their positional components for positional accuracy validation, producing a final map without trends in center pivot sizes and with accuracy adequate to the scale of 1:150,000, compatible with the resolution of the Landsat images.

The resulting yearly maps for Western Bahia were further processed at the ottobasin scale, to select only the highly irrigated regions, i.e., ottobasins with at least 4% of their total area irrigated in 2018. A total of seven regions were selected (gray areas in Figure 1.1).

1.2.4. Calculation of Regional Water Demand for Irrigation

The regional water uptake for irrigation depends on (1) the effective area irrigated at some time (A_I), in km^2; (2) the reference evapotranspiration rate (ET_o), in mm/day; (3) the crop being irrigated and its stage of development, which are integrated into an adimensional "crop coefficient" K_c, that usually varies between 0.3 and 1.3; and (4) the efficiency of the system (ε), which for center pivots is typically around 0.8. The water uptake for irrigation (Q_I) in $m^3\ s^{-1}$ is the product of these four terms:

$$Q_I = \frac{A_I\ K_c\ ET_o}{86.4\ \varepsilon}.$$

Although we have mapped all center pivots in these regions, our estimates of irrigated area should be understood in terms of area with installed irrigation systems. These systems may be used fully, partially, or not at all, depending on the year and the season. Currently, there are no regionally consolidated data of the actual amount of irrigated area nor the crops planted per center pivot as a function of time.

To overcome this limitation, we interviewed 20 irrigators and one irrigation consultant (who consulted for several tens of irrigators). Interviews were conducted between July 2018 and October 2018, either in person or by phone. We asked questions about the frequency of irrigated crops a year, typical planting dates, crops planted, amount of irrigation applied, and the main reasons why they make their management decisions.

1.3. Results

1.3.1. Changes in precipitation

Figure 1.3 shows the evolution of annual mean regional precipitation for the three basins. In addition, data for the Barreiras station are also shown. An analysis of Figure 1.3 indicates that two main characteristics of these time series stand out. First, annual mean precipitation presents strong interannual variability, ranging from ~600 to >1700 mm year^{-1}. In other words, individual precipitation years range from values typical of the semi-arid climate east of the region to values typical of the tropical seasonally dry climate west of the region. The interannual variability pattern is also consistent across the three basins, which indicates that it is large-scale driven. In addition, the regional pattern correlates well with the data at the Barreiras station, which allows for speculative interpretations in the period before 1980.

Second, basin-wide precipitation has not been greater than 1370 mm year^{-1} since 1992, while this level has been exceeded five times between 1980 and 1992, and another five times in the period from 1961 to 1979, if considering the Barreiras data. This is a major shift in the precipitation regime, that affects the regional decadal means. To be sure, we applied the non-parametric Pettitt´s test for detecting changing points to the region-wide 1980–2015 time series, which confirms a changing point at $\tau = 13$ (1992), with $K_T = 87$ and significance level 4.6×10^{-9}.

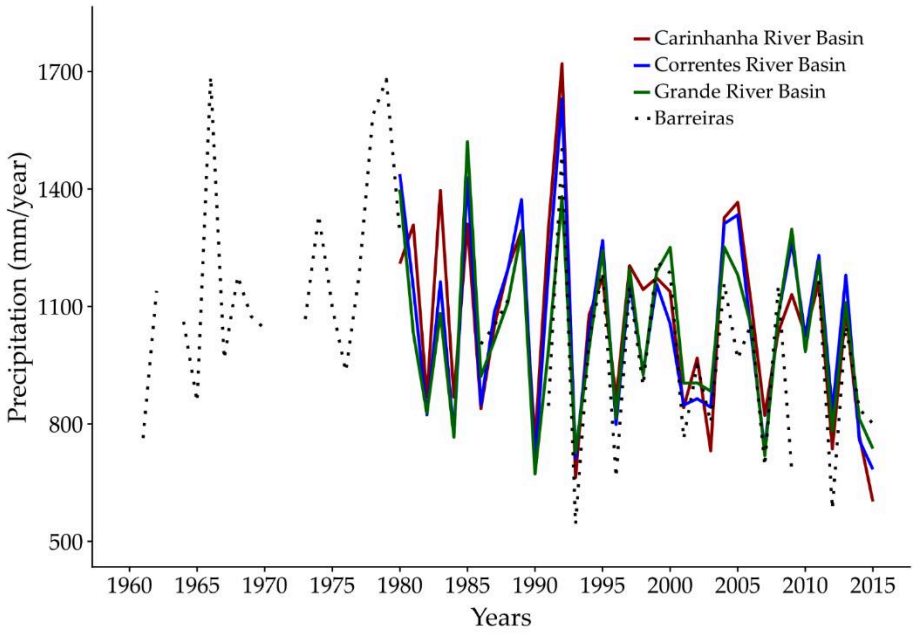

Figure 1. 3. Annual mean precipitation for the three basins and historical precipitation for the Barreiras rain gauge.

Based on this evidence, the 36-year time series of rainfall and river flow were divided in two periods, namely P1 (1980–1992) and P2 (1993–2015), to test the hypothesis of precipitation change between the two periods. We also tested other divisions of the rainfall time series (two periods of 18 years, three periods of 12 years), but the division in P1 and P2 was the choice that yielded the highest significance in precipitation change.

Indeed, the regional patterns of mean precipitation for the two periods (P1, P2) show that isohyets are moving westward from P1 to P2 (Figure 1.4a,b), translating into a regional drying from P2 with respect to P1 (Figure 1.4c). Although the period of analysis is relatively small, significant precipitation change has been detected. Extremely likely ($\alpha = 0.05$) precipitation reduction, averaging −165 mm year^{-1} (−12% compared to P1 mean), appears in a core area in the west of the region. This core area is surrounded by very likely ($\alpha = 0.10$) precipitation changes (Figure 1.4c), and average drier conditions throughout nearly all the region (Figure 1.4c). Moreover, the Mann–Kendall trend test indicates precipitation trends consistent both in sign and in significance with the precipitation differences (Figure 1.4d).

Considering basin-wide averages, the significant reduction in precipitation has happened mainly in the months with higher precipitation (December and January) in the three basins (Figure 1.5, $\alpha = 0.05$). In addition, the interannual variability of precipitation, measured

by both the interquartile difference and the range of variability, has also decreased in the three basins in P2, when compared to P1 (Figure 1.6).

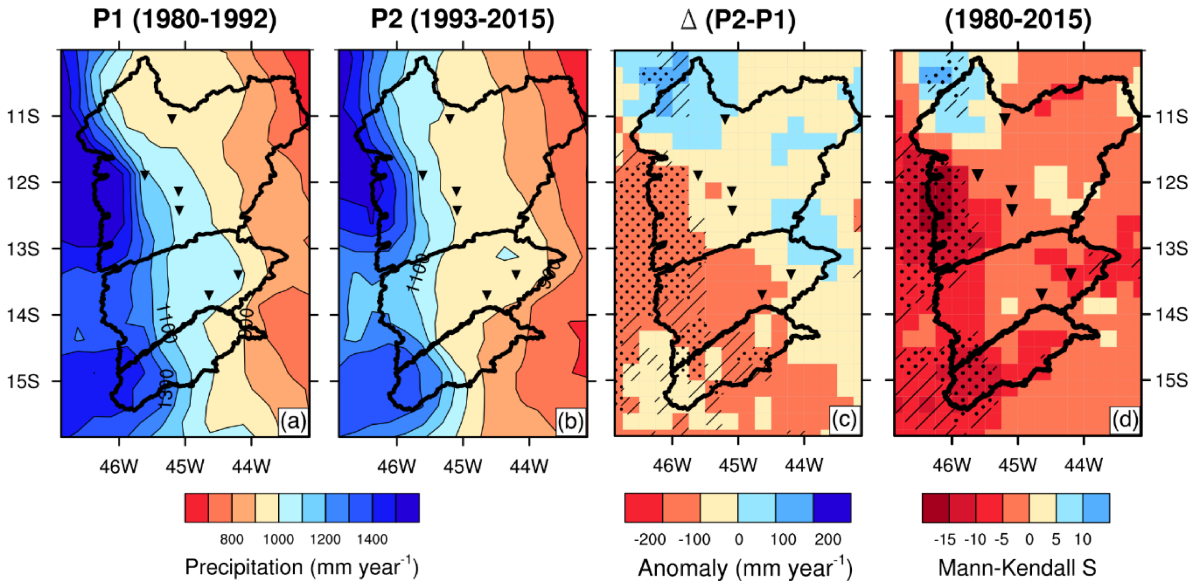

Figure 1. 4. Average precipitation map for periods P1 (**a**), P2 (**b**) the difference between P2 and P1 (**c**), and the Mann–Kendall S statistic (negative values represent decreasing trends). The six selected river flow stations are also shown. Dotted areas represent differences significant at $\alpha = 0.05$, according to Student´s t test (in **c**), or according to the Mann-Kendall test (in **d**), while shaded areas represent differences or trends significant at $\alpha = 0.10$.

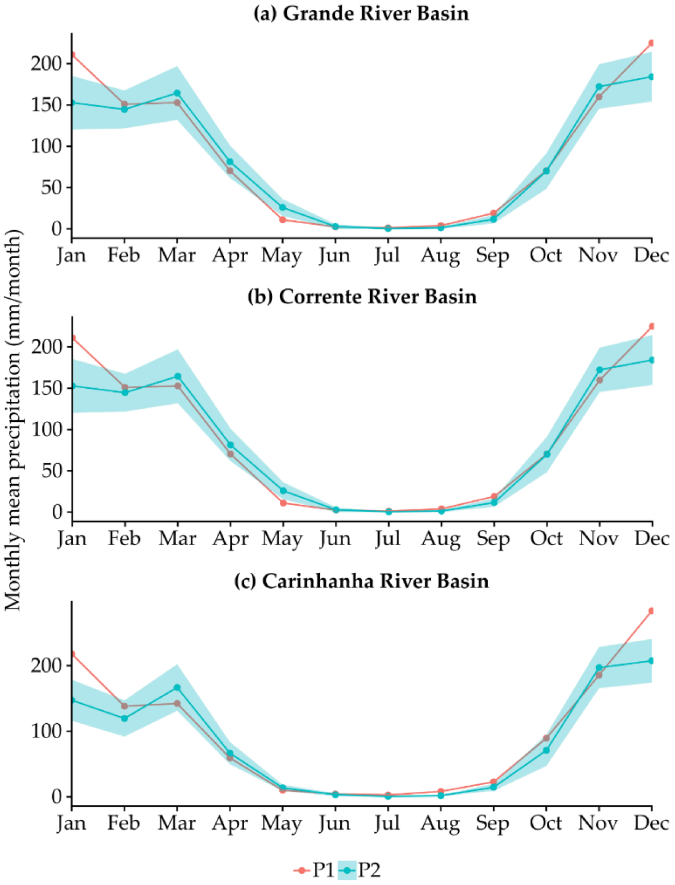

Figure 1. 5. Monthly mean precipitation for two periods (P1 and P2) for the three basins. The shaded area in P2 is the confidence interval for the mean (α = 0.05). Averages in P1 outside the shaded area are statistically different at this level of confidence.

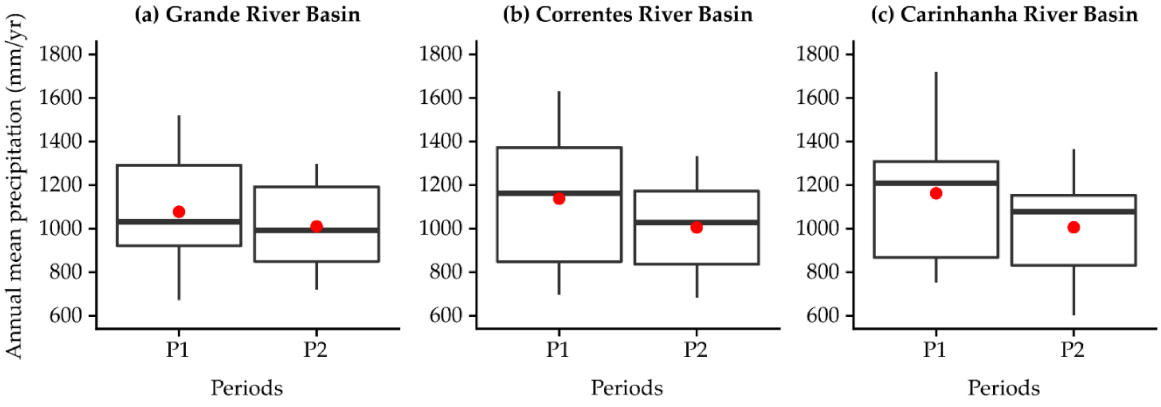

Figure 1. 6. Boxplot displaying the median (thick lines), the lower and upper quartile (box), the mean (red dots), and the minimum and maximum of the distribution (whiskers) for annual values of precipitation in periods P1 and P2. Period P1, although much shorter than P2, has higher interannual variability.

Two main large-scale systems are likely the cause of the reduced rainfall in this region, both linked to higher interannual variability and more extreme drought years (Marengo et al., 2017). First, the warming of the tropical North Atlantic Ocean leads to a higher frequency of anomalously northward positions of the intertropical convergence zone (ITCZ). In addition, changes in the temperature of the Pacific manifested as extremes of the El Niño-southern oscillation (ENSO) are partially associated with extreme drought in the region (Kane, 1997; Ambrizzi et al., 2004)).

We suggest that the strong interannual variability of precipitation is driven by the seasonal expansion of the subtropical high across northeast Brazil. In dry years (El Niño years and warmer North Atlantic years), it expands more to the west, reaching the Bahia/Tocantins border. In wet years (La Niña years and cooler North Atlantic years), it expands less, staying to the east of the São Francisco River.

1.3.2. Changes in River Flow

The flow duration curves for the six stations analyzed in this work are presented in Figure 1.7. These curves show the percent of time specified discharges were equaled or exceeded during each period (P1, P2). All panels show that discharge has been decreasing at all levels of probability.

The discharge of these rivers is heavily regulated by the Urucuia aquifer. Parallel flow duration curves, like Figure 1.7c–f, indicate that the decrease in discharge is mainly caused by the reduction in rainfall, and modulated by the aquifer. While a monitoring piezometer network of the aquifer was set up only in 2011, by 2015 it already shows groundwater level drawdown of up to 5 m (Marques et al., (2018).

On the other hand, when the decrease in discharge is smaller in the wet season (lower percentiles) and higher in the dry season (higher percentiles), which is the case of Figure 1.7b, this is an indication that withdrawal of water during the dry season may be playing a relevant role in the decrease of discharge. It is no coincidence that station B (also region R2 in Table 1.2) is the one among the six selected with the highest density of irrigation upstream (4.8% of the upstream area irrigated), while the other ones have less than 1% of their drainage area irrigated. We suggest that water withdrawal for irrigation is only detectable in fluviometric records when irrigation upstream is between 1% and 4% of the drainage area of the station.

In addition, it can also be verified in Figure 1.7 that nearly all discharge data recorded during P1 in these six stations are higher than Q_{90} of P2. This means that, even considering the

long term (1978–2015), Q_{90} is mostly defined by the discharges observed in P2 only. This is confirmed by Figure 1.8, which clearly shows that most of the situations when daily discharge Q is smaller than the long-term Q_{90} (LT Q_{90}) happens after 2000. In an extreme case, station D in a very dry year like 2015, 72% of the days (263 days out of 365) had daily Q lower than the LT Q_{90}. Although this is a severe case, it is relatively common to find years when more than half of the days are below the LT Q_{90}.

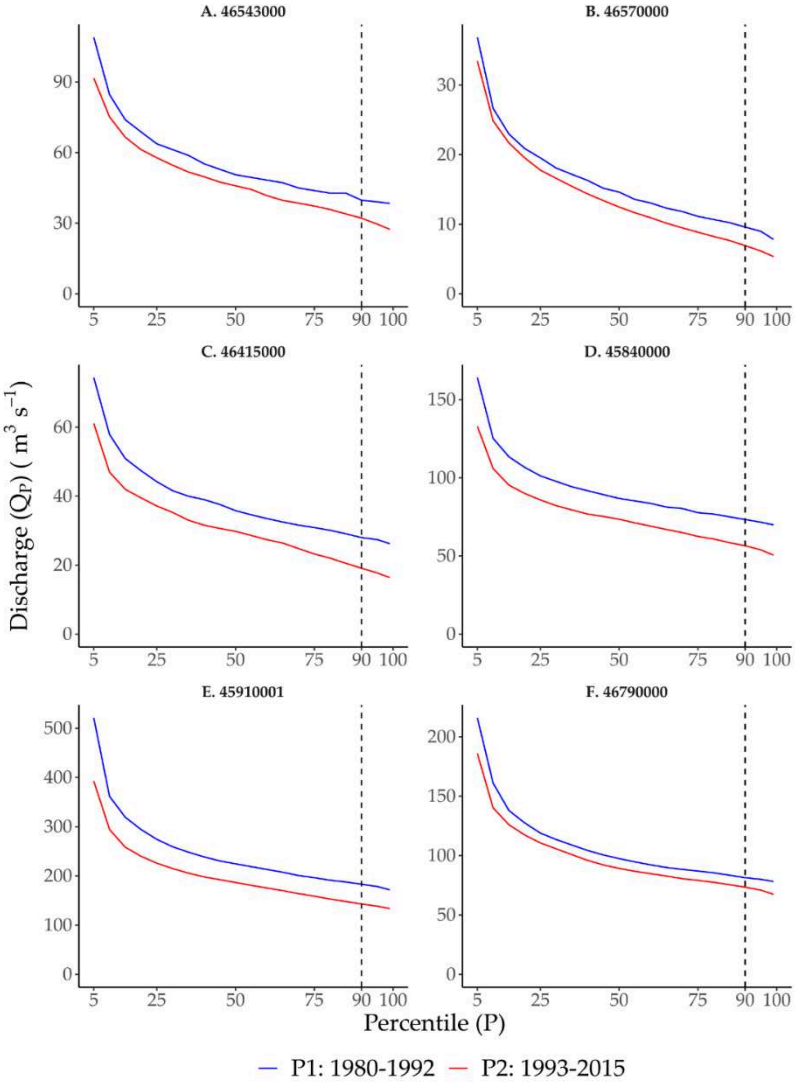

Figure 1. 7. Flow duration curves for stations A–F for periods P1 and P2. Values in the x-axis are the probability that a given discharge (Q_p) is exceeded during that period. The intersection of the dashed line, representing the 90% percentile, and each curve, represents the Q_{90}.

Our interpretation of these data is that, even if considering its relatively short (38 years) duration, all river discharge time series are non-stationary. Discharge has been decreasing all over the spectrum and throughout the region, minimum discharges have been defined in the most recent years, and even when the most recent dry years have been considered for the

definition of minimum discharges, the actual recent rate of occurrence of a relatively unlikely phenomenon like $Q < Q_{90}$ is four to seven times higher than the expected probability. Under these circumstances, probability discharges cannot be used to predict the distribution of future flows. In addition, although the results are not shown here, the above characteristics are consistent across 24 of the 25 stations analyzed, except the northwesternmost station (upstream of station F), only area where precipitation did not decrease.

Non-stationarity can be explained by several factors, such as changes in river basins by anthropogenic effects, climate change, and low-frequency climate variability (Bayazit et al., 2015). Moreover, this does not seem to be the case of uncertainty dominating the distribution of extremes, as suggested by Serinaldi and Kilsby (2005). The entire flow duration curve has shifted down, not only the extreme values. This is very much consistent with the picture of rivers regulated by a decreasing-level aquifer, following a reduction of the aquifer recharge after reductions in precipitation, arguably caused by a strengthening of the South Atlantic subtropical high-pressure system associated with the warming of the North Atlantic and Central Pacific, the ultimate causes for the non-stationarity. This is our current reasoning for the attribution of causes, although it can only be verified through detailed hydrogeological modeling and large-scale climate dynamics studies, which are beyond the scope of this work.

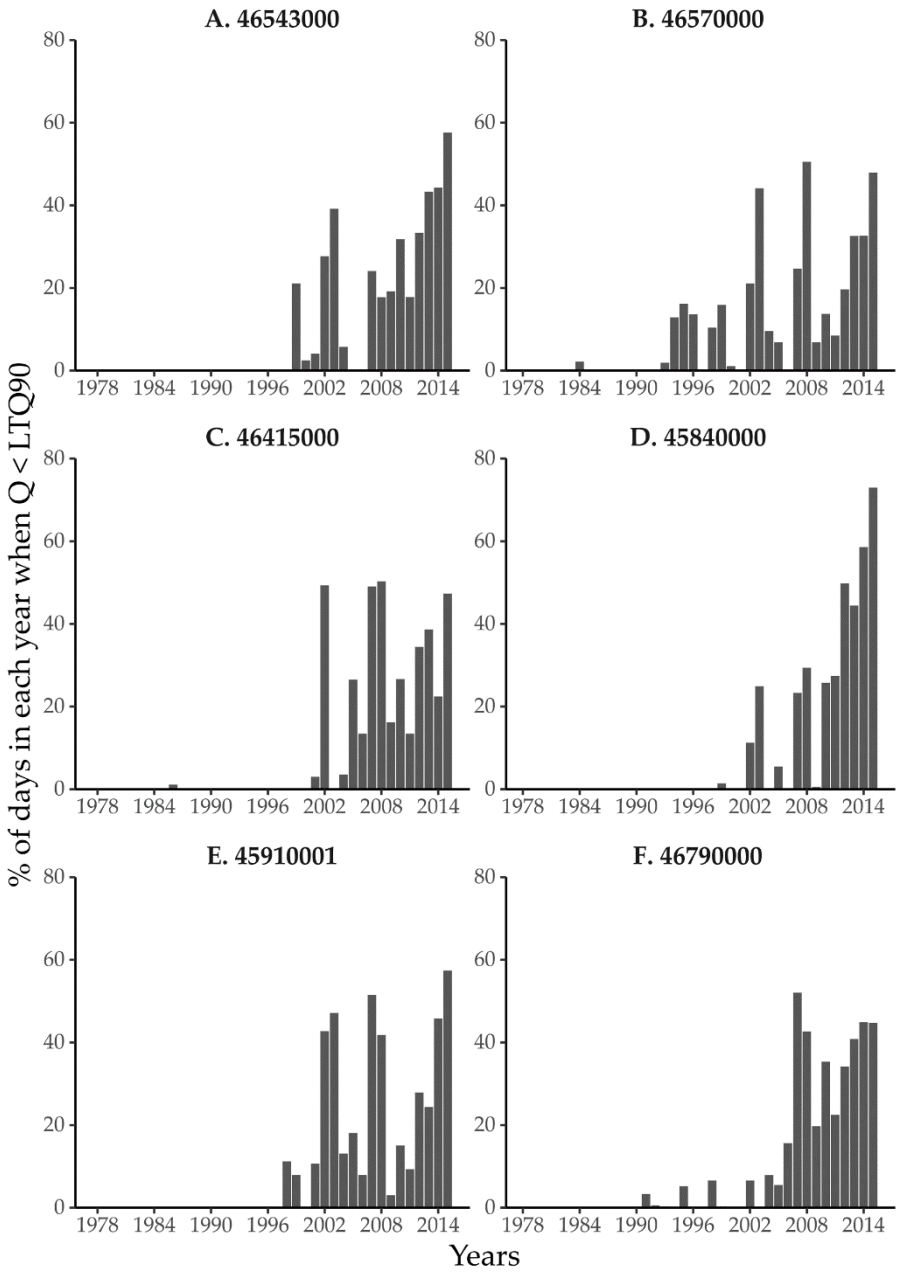

Figure 1. 8. Percentage of days in each year when actual Q is below the long-term Q_{90}. Long-term Q_{90} is calculated for the period 1978–2015. The concentration of cases of Q < LT (long-term) Q_{90} after 2000 indicates drastic reductions in minimum discharges.

1.3.3. Trends in Irrigated Area and Water Uptake on the River Flows

To evaluate the effects of irrigation water uptake on the river flows, we choose seven regions with the highest concentration of irrigated area, where these effects are expected to be most significant. These seven regions have between 4.8% and 12.6% of the area of the ottobasin irrigated, while no other ottobasin in the region has more than 4%. The spatial evolution in irrigated area in these regions (R1 to R7) is shown in Figure 1.9. The total irrigated area in these

seven regions was 662.4 km^2 in 2010, which increased to 1256.1 km^2 in 2018, a 90% increase in just eight years (Table 1.2). Figure 1.10 shows the temporal evolution of irrigated area for each region. Each region has a different pattern of growth, but all regions show a substantial increase in irrigation since the 1990s.

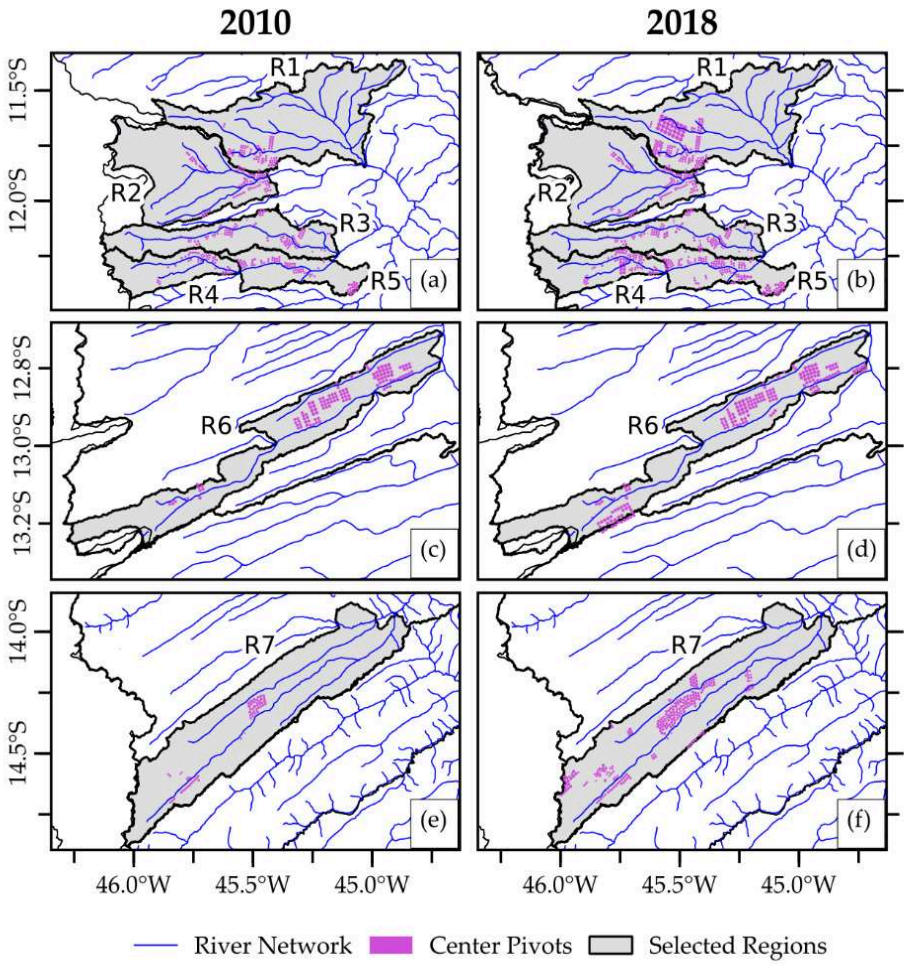

Figure 1. 9. Evolution of irrigated area for selected regions for 2010 and 2018. Each center pivot ranges from 26.9 ha to 355 ha in area. The North–South scale of (**c**) and (**d**) is different than the same scale of (**a**), (**b**), (**e**), and (**f**).

Table 1. 2. Selected regions (R1–7) where irrigated area is located in Figure 1.9, with corresponding ANA Ottobasin codes. The region R2 coincides with the drainage area of station B.

Region (Ri)	ANA Ottobasin Code	River	Total Area (km^2)		Irrigated Area in 2018		
			Ottobasin	Region	Ottobasin (km^2)	Region (km^2)	% of Total Area
R1	76243	Rio Branco		3403.5	232.9	232.9	6.8%
R2	46570000*	Rio de Janeiro		2522.1		122.2	4.8%
R3	762641	Rio Cabeceira de Pedras		1739.6		108.6	6.2%
R4	762691	Rio Borá		938.3		89.2	9.5%
R5	7626711	Rio de Ondas	778.64	1939.2	121.1	244.2	12.6%
	762661	Rio de Ondas mouth	222.33		33.9		
	762691	Rio Borá (upstream)	938.3				
R6	762891	Rio Grande	197.10	2075.2	42.0	194.7	9.4%
	76489	Rio Guará	295.04		11.1		
	762871	Rio Grande	361.45		42.1		
	76285	Rio Grande	789.94		37.2		
	76282	Vereda Passaginha	431.66		62.3		
R7	764271	Rio Pratudão	662.35	3865.0	14.3	264.2	6.8%
	76426	Riacho do Váu	702.94		115.0		
	764241	Rio Formoso	2499.73		134.9		

* Represents the fluviometric station code.

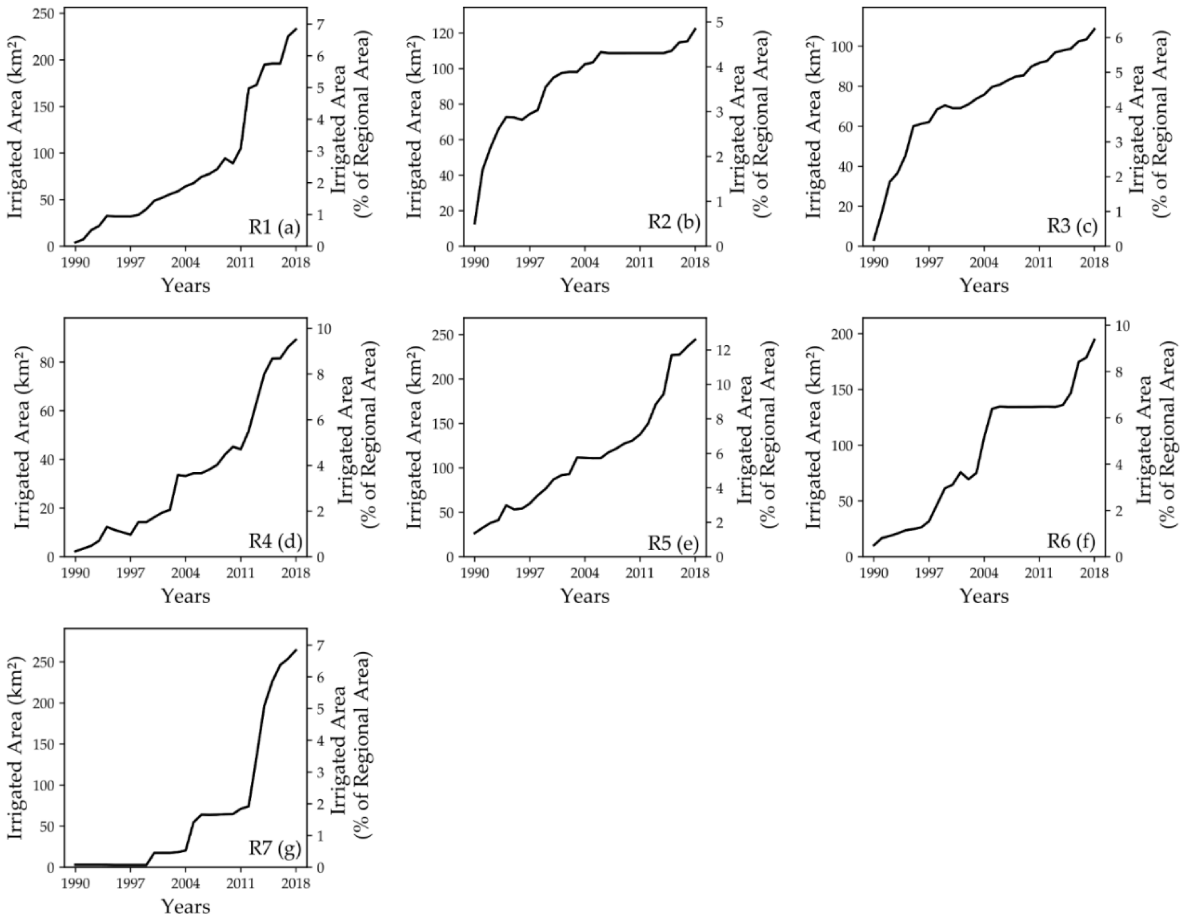

Figure 1. 10. Evolution of irrigated area in selected regions, as defined in Figure 1.9 and Table 1.2.

With the area irrigated estimated and the areas with intense irrigation growth identified, in order to calculate water uptake, information on water demands per unit area are still needed (Section 2.4). From the interviews conducted, during the driest period of the year (September and October), when river discharge approaches Q_{90} values, water application rates ($K_c\ ET_o/\varepsilon$) could be as high as 10 mm day^{-1}, if the irrigator had a high consumption crop like maize at the peak of the cycle (K_c ~1.3); at the same time, when ET_o is very high, because cloudiness is low, incoming solar radiation is at a yearly maximum and relative humidity is low. However, this is a highly avoided situation by irrigators, because of the high costs of energy in September and October.

The electric energy fares in most of Brazil are flagged (green, yellow, or red) according to the actual costs to produce energy in the country. In 2017, on an annual mean, 63.8% of the electricity generated was hydroelectric, 17.2% was produced from fossil fuels sources, other renewables (biomass, solar, and wind) accounted for 17.6%, and nuclear participated with 1.3% (MME, 2019). Hydroelectricity is usually much cheaper than the other sources, and its availability is also seasonal. So, during the end of the rainy season, when reservoirs are at the

highest level, proportion of hydroelectricity increases and costs decrease (green flag), while at the end of the dry season (September and October), when reservoirs are at the lowest level, proportion of fossil fuels (and costs) increase, leading to the red flag tariff (*Bandeira vermelha*). Although this is the general pattern, other factors, like interannual variability of rainfall, and any other significant changes in supply or demand may also affect the flagging, which is updated monthly.

If the irrigators generally avoid having high consumption of water during the driest months, what management do they usually practice at this time of the year? The results of our interviews indicate that the most common situations are either to have a crop at the end of the cycle when K_c is small (~0.65), or to have the crop cycle (and irrigation) finished by this time of the year.

We then consider two scenarios of regional water management for these seven regions, an aggressive one and a conservative one. In the aggressive scenario, maximum crop output is emphasized; regionally, irrigators would be planting year-round crops (either perennial crops like coffee, or sequential seasonal crops, like soy, cotton, maize, or beans); if sequential seasonal crops, one of the crops would be at the end of the cycle in September and October (K_c = 0.65), demanding on average 5 mm/day (150 mm/month) for all areas with irrigation systems installed; and irrigators plan to sow the next crop after the onset of rains in late October or November. The conservative scenario assumes that one-third of the irrigated area is cultivated with only two crops a year, and there is no irrigation during the driest months (K_c = 0); two-thirds of the irrigators still act aggressively, as in the previous scenario, some of them because they grow perennial crops and must irrigate year-round; all farmers still plan to sow the next crop after the onset of rains in late October or November, to minimize the costs of energy. Regional irrigation in this conservative scenario is the weighted average of the irrigation levels ($1/3 \times 0 + 2/3 \times 150$), or 100 mm/month.

Again, these are scenarios based on the declared experience of the local people. So far, there are no public yearbooks that document month-by-month variations in planted area, just snapshots of irrigated area that do not capture the quick growth of irrigation systems in the region, neither the seasonality, nor the timing of irrigated crops. In a future work, we plan to use remote sensing to estimate the actual amount of irrigated area and the irrigation period per center pivot as a function of time.

Water uptake for irrigation (Q_I) was estimated from the multiplication of the total area irrigated by the water application rates in the two irrigation management scenarios. Evolution

of Q_I from 1990 to 2018 is shown in Figure 1.11, for regions R1 to R7. Discharge measurements are not available for these regions (except for R2, which will be analyzed again in Figure 1.12), so we use regionalized values of Q_{90} (Oliveria et al., 2019). This technique is a downscale of discharge for drainage areas smaller than the available measurements, using empirical equations based on independent variables like area upstream or average precipitation upstream. These authors tested several empirical relationships, and the best skill low streamflow regionalization was obtained by basin-specific regression equations of Q_{90} against the upstream long-term annual rainfall minus an initial abstraction of 750 mm ($P_{eq750} = P - 750$) as independent variable (Pruski et al., 2015).

Figure 1.11 plots 80% of long-term Q_{90} (the maximum discharge that could be granted for all human use, including irrigation). A water use conflict situation appears when the demanded water resources (blue or green lines) are higher than the availability of water resources (horizontal dashed red line). The aggressive scenario (blue line) implies conflicts in regions R1, R2, and R4. In the Rio de Janeiro region (R2), at least since 1997, these conflicts may have been sporadically occurring, depending on year-by-year decision to irrigate in the low flow months. This helps explain why the installation of center pivots has been halted between 2005 and 2013 (Figure 1.10b). Conflicts, however, may be avoided by a community decision to follow the more conservative scenario, which tolerates additional increases in irrigation area, as observed after 2015 (Figure 1.10b).

In R3 and R5, although the estimated demand of water resources has not yet reached the limit of 80% LT Q_{90}, they all show a quick increase in the use of water, and if the rates of irrigation growth continue to be high, water conflicts are imminent. In regions R6 and R7, although imminent conflicts may be in principle discarded, conflicts may still arise in the timescale of a decade or two, if irrigation growth rates remain high.

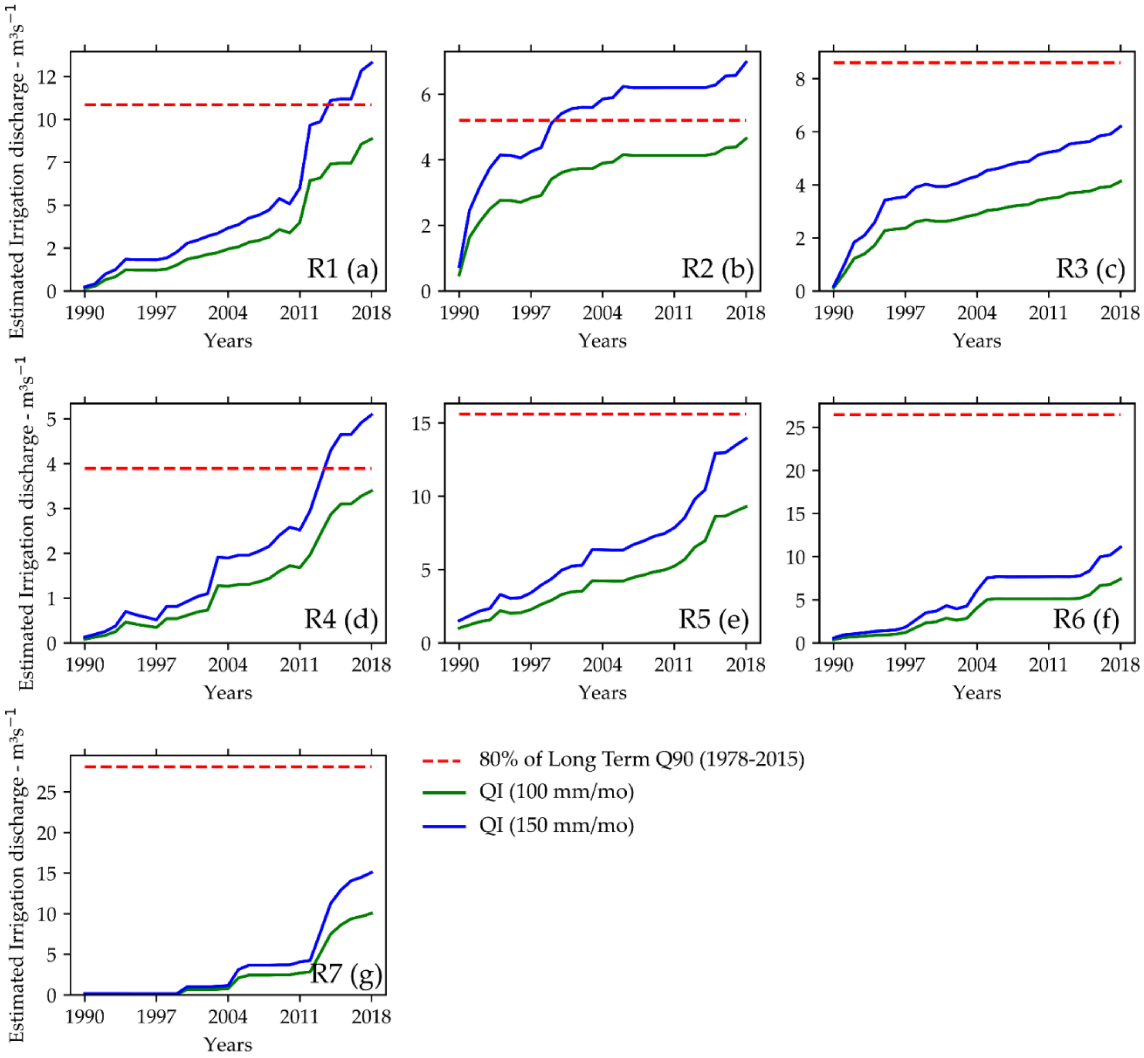

Figure 1. 11. Scenarios of discharge uptake for irrigation in selected regions, assuming two water application rates (100 and 150 mm/month). 80% of long-term Q_{90} is the maximum river discharge that can be granted permission for human use (Verstraeten et al., 2006).

The intense growth of irrigation systems (90% from 2010 to 2018, Table 1.2) is hardly the only concern for water users in Western Bahia. As described in Figure 1.7, the safe discharge for concession of water use permits, Q_{90}, has decreased everywhere in the basin. Q_{90} is mostly defined by the discharges observed in P2 only, which covers the period 1993–2015, so the use of updated hydrological information is crucial to minimize the hydroclimatic risks (Figure 1.8). In fact, Figure 1.12A–F does a similar water conflict analysis for the six selected hydrological stations. Of those, four (Figure 1.12A–D) have much irrigation upstream, while two of them (Figure 1.12E,F) have little irrigation upstream. A remarkable feature of Figure 1.12 is the decrease of Q_{90}, calculated only with data for P1 and only with data for P2 (black dashed lines).

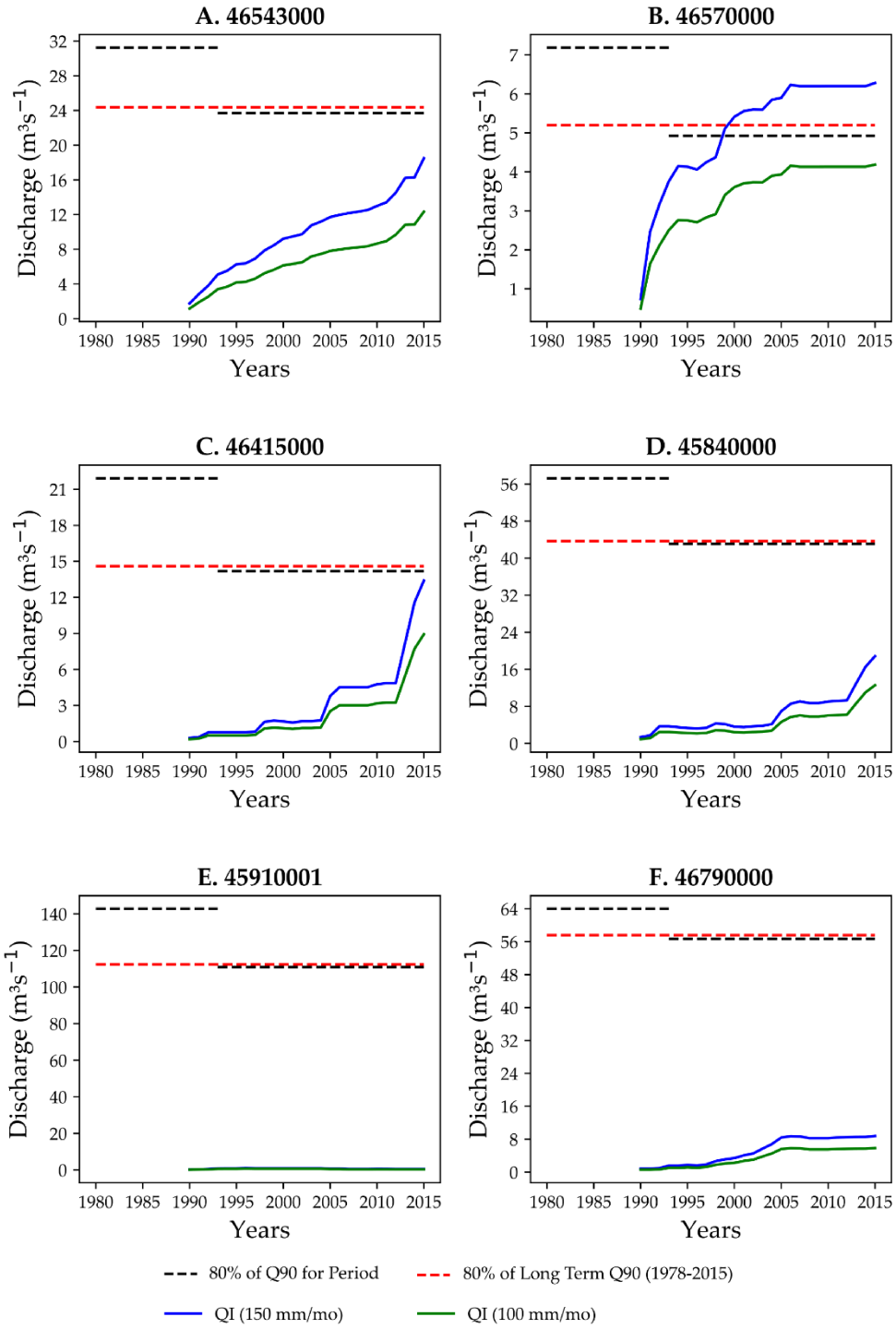

Figure 1. 12. Evolution of discharge uptake for irrigation (QI) in the drainage area of each river flow station, assuming two water application rates (100 and 150 mm/month). 80% of long-term Q_{90} (dashed red line) is the maximum that can be allocated at that point. The black dashed lines represent the change in the availability of water resources from P1 to P2.

1.4. Discussion and Conclusions

1.4.1. Climate Change and Intense Irrigation Growth: Increasing Water Stress

An analysis of Figure 1.12A–D indicates that conflicts of water use may arise much sooner if outdated hydroclimatic information is used to define water granting rights. For example, a hypothetical Q_{90} defined using only pre-1992 data is between 15% and 60% higher than the Q_{90} calculated when the more recent years are considered (black dashed lines). Following the non-stationarity of the time series, the long-term Q_{90} (1978–2015) nearly coincides with the recent, shorter-term (P2) Q_{90} everywhere in the basin. In particular in Station B, which is coincident with R2, as early as the late 1990s, irrigation water demands, probably granted based on data of a wetter period, were no longer consistent with the decreasing availability of water resources. This inconsistency was probably understood in 2003, when discharge was low (below long-term Q_{90}) during 45% of the year (Figure 1.8b), leading to a halt in the installation of new center pivots in the area shortly after (Figure 1.10b). However, since 2015, irrigated area in the region has resumed its expansion, which is of much concern (Figure 1.10b). Water withdrawn for irrigation certainly affects the measurements, in particular in regions with a high density of irrigation systems like the sub-basin upstream of station B. This effect, however, is reduced in the other stations, which have a smaller density of irrigation systems.

At least seven sub-basins in Western Bahia are either in a state of conflict for the use of water or are moving rapidly towards it: Rio Branco, Rio de Janeiro, Rio Cabeceira de Pedras, Rio Borá, Rio de Ondas, Rio Grande (headwaters), and Rio Formoso. These sub-basins account for 17% of the area of Western Bahia. In these seven critical sub-basins, water conflicts are imminent, if irrigators actually irrigate in the driest months of the year, when discharge usually gets around or below Q_{90}. As a short-term alternative, conflicts can be avoided if irrigators largely avoid irrigation during these months. As shown in Figure 1.8, this is not restricted to a few months of the year. In many dry years, nearly half of the year daily discharges were below Q_{90}, with an extreme case in station D (Formoso river) in the very dry year of 2015, when daily Q was below Q_{90} during 72% of the year. To be sure, such Q_{90} already includes 2015 data.

Because of the declining rains and water resources, the water resource concession limits (80% of LT Q_{90}) may be reached with a much higher frequency than originally planned if outdated hydroclimate information is used. The combination of strong increase in demand of water for irrigation and the maintenance of low flows may bring much more critical

consequences for water management in the region in the next years. Here, we discuss four different pathways to reduce water stress and increase water security: (i) Avoid irrigation during the low flow period; (ii) halt the installation of new irrigation systems; (iii) bet on a return to wet conditions; and (iv) invest in a hydroclimatic monitoring system.

1.4.2. Avoid Irrigation During the Low Period

Avoiding irrigation during low-flow periods can be achieved by planting only two crops a year, one from November to February, and a second one from March to June. This is the most natural reaction to improve water security. This practice maximizes the use of rain during the six-month rainy season and cuts the use of irrigation to typically two months, reducing the water consumption not only because of the short irrigation period, but also because of the low ET rates at the end of the cycle. In addition to increasing water security, this practice also reduces production costs by avoiding the high costs of energy during the end of the dry season in Brazil, when additional energy tariffs (*bandeira vermelha*) are charged.

On the other hand, this practice has several drawbacks. Multiple cropping increases the revenue per plot, provides diversification of income, reduces pest pressure, and helps to maintain a more stable pool of farm labor, avoiding seasonal unemployment and the related social consequences (Richards et al., 2015). It is also an important factor in the intensification of land use, which, if combined with additional conservation measures, reduces the pressure to expand cropland at the expense of natural ecosystems, possibly sparing land from deforestation. Moreover, this practice is not applicable on perennial crops.

1.4.3. Halt the Installation of the New Irrigation Systems

Halting the installation of new irrigation systems, either through a ban of new water permits or by collective irrigators decision, is a short-term measure that vigorously attacks the problem from the viewpoint of the increasing demand. As stated earlier, this alternative has been requested by the Rio Corrente Basin Committee as a precautionary measure.

This option, however, does not resolve the conflicts of the regions already under a state of conflict, in particular in the Rio Grande basin, where the water demands are already too high in some places. It also does not address the problem of decreasing water availability. In addition, there are the economic consequences on jobs, tax revenue, and economic growth.

Although severe, it may be necessary in some regions with very high demands, in particular if the minimum discharges continue to decrease. A constant update of the low discharge values would be desired in this case.

1.4.4. Bet on A Return to Wet conditions

The third alternative is to consider that current low precipitation period is not permanent and climate will return to the pre-1992 wet state.

Given the low skill of the current generation of interdecadal climate prediction models (Kirtman et al., 2013), it is hard to forecast whether these reducing precipitation trends will continue in the next decades. As said before, the location of Western Bahia in the transition between the semi-arid and the seasonally dry tropical climate regions makes it a serious candidate for climate change. CMIP5 simulations indicate a strengthening of the South Atlantic subtropical high, with a reduction of precipitation in the semi-arid of Northeast Brazil, and a possible expansion of the semi-arid climate over the region with a current seasonally dry climate (Magrin et al., 2014). This expansion, however, is somewhat uncertain given the relatively coarse resolution of the climate models involved in the CMIP5 ensemble (from 1.1° to 2.8°), when compared to the east–west dimension of the region (~2.5°). Despite the low skill of these models, the most likely scenario for the 21st century, as simulated by the CMIP5 ensemble, is an additional drying of the region, in particular in the months of September, October, and November, with very high agreement among models (Marengo et al., 2017)

In addition, because the local rivers are connected to the Urucuia aquifer, pre-1992 river discharge levels may only be resumed after the aquifer previous levels of storage are restored, which may take from several years to several decades—our current understanding of the coupling of the aquifer and the rivers of the region is not sufficient to answer this question more precisely. Moreover, since the aquifer water level monitoring network was only set up in 2011, we do not know what the state of the aquifer was during the wet climate period.

In summary, climate models do not support a return to wet conditions—on the contrary. Even if climate models drying predictions do not materialize, it may take several decades to return to former conditions. Betting on this is a risky alternative.

1.4.5. Invest in A Hydroclimatic Monitoring System

The three alternatives discussed earlier may mitigate water conflicts, but all have their setbacks and risks. Western Bahia is an agriculture frontier under constant change, lacking a crucial element for management: Data. As stated earlier, the water resource management based on the long-term probability of hydroclimatic events requires at least a constant update of the low discharge values. But this does not seem to be sufficient. In the most water-stressed regions described above, a true management, in which the availability and demand of water resources

for irrigation are actually measured and monitored, is the safest path to provide water security to this region. Such a monitoring system will allow a more confident and sustainable regional management of irrigated agriculture, maximizing the use of water resources, food production, and economic development, while reducing the risk of water conflicts.

This monitoring system should have three components: (1) Measurement and short term reporting of river discharge at key points in these basins, in particular in the sub-basins where the concentration of irrigation areas is higher; (2) a hydroclimatic forecast system to predict the availability of water resources at the period of lowest availability (September and October) several months in advance, in order to influence the irrigator decision to conduct an irrigated crop and when to plant this irrigated crop; and (3) monitoring and short-term reporting of the actual consumption of water for irrigation at the sub-basin scale. The latter can be done using either one of three possibilities: (i) Installation of hydrometers at each pumping station; (ii) correlation of water consumption with energy consumption, and monitor the latter; and (iii) monitor the actual evapotranspiration through operational remote sensing products, such as the MOD16 evapotranspiration product, correctly calibrated with field data for a reliable representation of reality. These measurements must be integrated at a monitoring center, which would periodically issue recommendations of how much area can be irrigated that year.

1.4.6. Final Remarks

It has been argued that water crises are mainly crises of governance (UNESCO, 2006). Governance is a more inclusive concept than government itself, embracing the relationship between a society and its government. Governments mediate behavior through institutions, policies, laws, norms (like issuing water permits), and actions (like fiscalization and enforcement), but governance also relates to domestic activities, networks of influence, international market forces, the private sector, and civil society (Roger et al., 2003). This concept has been incorporated by the Brazilian Policy on Water Resources (Law 9433 of 8 January 1997), which states that management of water resources must be decentralized with the participation of the government, users, and communities. The suggested monitoring system would provide the regional stakeholders (government agencies, agribusiness, and organized civil society) with the necessary data and decision-making tools to make key decisions.

One such key decision is the determination of how much area may be irrigated at each ottobasin in each year, a critical decision in this region with very high interannual variability of rainfall. The correct decision of how much area to be irrigated each year, according to the

estimated availability of water resources, may contribute to avoid water use conflicts during the low water season, providing water security for both large irrigators and small farmers. If used wisely, it may also promote the long-term planning of the sustainable expansion of irrigation in the region, supporting the increase in the production of food, feed, and fiber, improving food security as well as water security.

CHAPTER 2. INTERACTIONS BETWEEN LARGE-SCALE AND MESOSCALE PROCESSES DEFINE LONG-TERM RAINFALL VARIABILITY AND AVAILABILITY OF WATER RESOURCES IN WESTERN BAHIA, BRAZIL

2.1. Introduction

The climate of Northeast Brazil (NEB) has long been considered one of the world's problem climates (Trewartha, 1961). Its geographical position near the equator (Figure 2.1) would suggest a rainfall distribution typical of equatorial regions. Yet, the annual long-term rainfall in the region is less than 800 mm/yr, typical of a semi-arid climate.

The impact of the dry climate and its interannual variability on social and economic life, policy, water security, and conflicts over water use in the region is huge (Cunha, 1902; Sampaio Ferraz, 1950). Since the 1920s (Sampaio Ferraz, 1925), several works have studied the causes of the abnormal drought climate in the region. Walker (1928) and Bjerknes (1969) hypothesized a relationship between the Southern Oscillation and the rainfall in NEB, i.e., a relationship to the Pacific Ocean Sea surface temperature (SST). Later, Hastenrath and Heller (1977) and Moura and Shuka (1981) found that SST anomalies over the Tropical Atlantic and rainfall/droughts in NEB are correlated with the occurrence of cold/warm SST anomalies in the north Atlantic (Kayano and Capistrano, 2014).

While the key to understanding the semi-arid climate of NEB is the oceans SST, the interannual rainfall variability in NEB is explained by multiple factors. In addition to ENSO, another major factor that explains the rain on the NEB is the Intertropical Convergence Zone (ITCZ) position, which is modulated by the variability of the Atlantic Tropical SST, especially by the North and South Atlantic dipoles (Kayano et al., 2016).

On the interdecadal scale, the Atlantic Multidecadal Oscillation (AMO) also plays a role. Folland et al. (1986) showed for the first time that there was a strong relationship between long wet and dry periods in the African Sahel with the SST anomalies. These anomalies are relative changes between the hemispheres on a scale of several tens of years but are explicit the Atlantic. The AMO is one of the most important climatic variations on this scale and is also known for the variation of the SST throughout the North Atlantic (Knight et al., 2006; Wang and Zhang, 2013). The AMO is divided into the warm (positive) and the cold (negative) phases in the Atlantic Ocean. During the positive phase, the SST is warmer throughout the North Atlantic and possibly cooler than normal in the South Atlantic. This phase increase energy release in the North Atlantic, favoring: the formation of hurricanes in the Caribbean Sea, wetter summers in northern Europe, heavy rains in the Sahel and African desert, drought years in NEB, and

reduction of Arctic Sea ice. In the negative phase, where the North Atlantic SST patterns are cooler and the South Atlantic SST patterns warmer, the effects are typically the opposite of the positive phase. (Delworth and Mann, 2000; Knight et al., 2006; Knudsen et al., 2011).

While there is some support for this mode in models and historical observations (McCarthy et al., 2015), controversy exists regarding whether AMO has a typical timescale and should be classified as an oscillation. Hence, it is also called Atlantic Multidecadal Variability (AMV). There is also discussion on the attribution of sea surface temperature to natural or anthropogenic causes (Mingfang et al., 2009; Enfield and Cid-Serrano, 2010; Mann et al., 2014; Li et al., 2020).

Several works have studied the relationship between NEB multidecadal climate variability and AMO. Knight et al. (2006) suggest that the ITCZ position favors precipitation over NEB during the AMO cold phase. Kayano et al. (2016) classified the wet and dry periods in NEB with the AMO phases for over 100 years (1901-2006), concluding that the percentage of dry years is greater during the warm phase. The opposite occurs in the cold phase. For the more recent period that included both cold and warm AMO phases (1981-2019), Shimizu et al. (2021) found decreasing precipitation trends in NEB with a change in the Walker and Hadley circulation.

The transition between the Cerrado climate and the NEB semi-arid climate is highlighted in Figure 2.1. To the west, the Cerrado biome has a six-month rainy season, from mid-October and mid-April, with annual precipitation > 1200 mm $year^{-1}$ (CGEE, 2016; Pousa et al., 2019; Vieira et al., 2021). In the middle of NEB, the semi-arid Caatinga is the predominant biome, with annual precipitation < 800 mm $year^{-1}$.

The Western part of the state of Bahia (red contour in the inset in Figure 2.1) is located in the transition climate. One of the most active agricultural frontiers of the world thrives in the region (Pimenta et al., 2021). The rainfall maximum at around 12°S-46.5°W (Figure 2.1, further explained later) is a fundamental characteristic for agriculture in the region. With abundant water available, the region has experienced rapid changes in land cover and land use for cropland, especially soybean, since 1985 (Pousa et al., 2019). Since 1990, yields have been increasing with the adoption of modern agriculture technologies. Cropland area reached 3.43 million hectares in 2020, with 218,000 irrigated hectares. Soy production in Western Bahia in 2018 amounted to about 6 Mt, roughly 5% of the nation's output, of which over 70% was exported. In addition, the cotton area in Western Bahia in 2019 amounted to 316,900 ha, roughly 20% of the nation's harvested area (Pimenta et al., 2021).

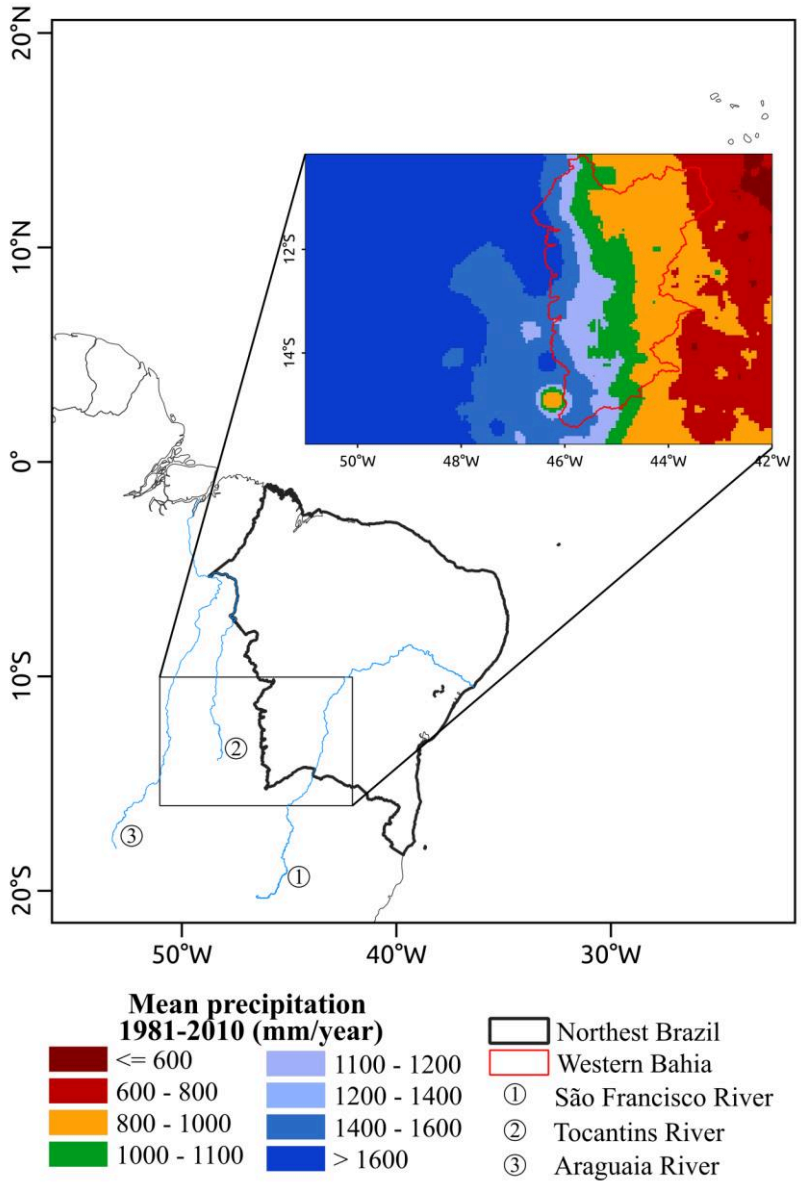

Figure 2. 1. Northeast Brazil and the variability east-west cross-section gradient in mean precipitation (1981-2010).

Figure 2.2 shows Western Bahia in detail. The region comprises three river basins (Rio Grande, Rio Corrente, and Rio Carinhanha), all tributaries of the São Francisco River, and is located on the top of the Urucuia aquifer. As shown in Figure 2.1, the region presents decreasing precipitation pattern from west to east.

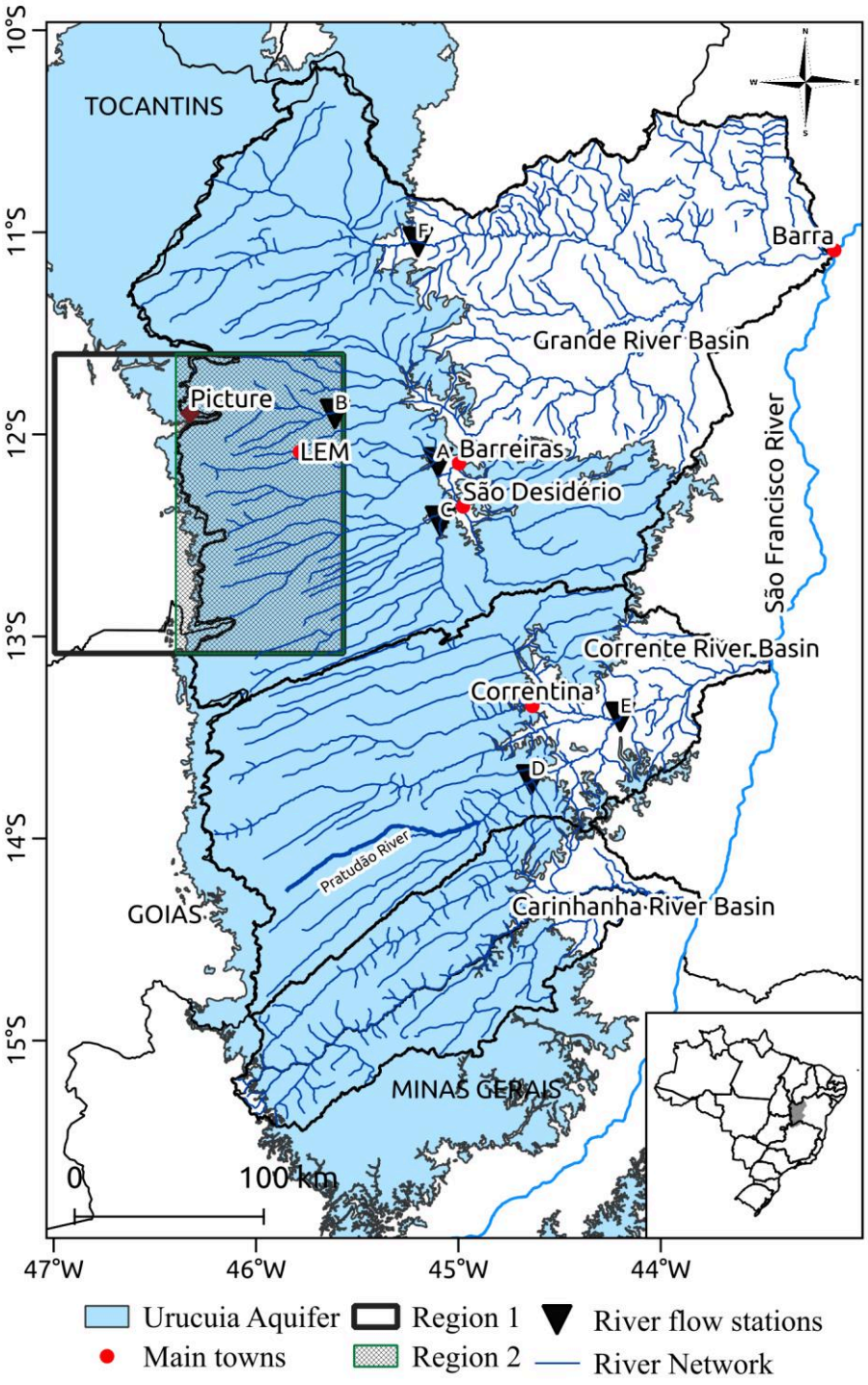

Figure 2. 2. Orientation map. Western Bahia and its three main watersheds (Grande, Corrente, and Carinhanha). The Urucuia aquifer (blue area) and the location of the main towns are also shown. LEM is the town of Luis Eduardo Magalhães. The thick-line and the shaded rectangles represent Regions 1 and 2 (R1 and R2), the areas for the main analyses. The picture point represents the point where Figure 2.4 was taken. A-F are the locations of the river flow stations described in Table 2.1.

The rivers in Western Bahia are regulated by Urucuia Aquifer System (UAS) (Pousa et al., 2019; Marques et al., 2020). Several factors control the variability of the interaction in rainfall-groundwater-surface water, such as rainfall patterns, land cover and land use, and topography (Marques et al, 2020). Of the controlling factors, the topography has a crucial role in the transition of precipitation patterns for the region. At 12°S, from east to west, topography increases from about 400 m above sea level (a.s.l.) at 45°W to over 800 m a.s.l., forming the regionally-called *Chapada* (Figure 2.3a). Then, a steep elevation difference around 46.3°W, the *Serra Geral de Goiás*, divides the states of Bahia from the states of Goiás and Tocantins (Figure 2.3a, Figure 2.4).

Region 1 (R1, Figure 2.2) represents the region where precipitation is under the strongest influence of orography. Considering the transect of 11.5°S-13°S, 51°W-44°W (Figure 2.3b), the typical west-east decreasing precipitation pattern dominates (Figure 2.3c). However, between 51°W to 46.4°W, rainfall diverges from the zonal gradient, locally increasing to a peak around 1500-1600 mm yr^{-1}, before it quickly decreases again to < 1000 mm yr^{-1} at 44°W (Figure 2.3c). See also the rainfall maximum at 12°S-46.5°W in Figure 2.1. The western part of R1 drains to the west, where conditions are wetter, while Region 2 (R2) represents the subset of R1 that drains to the east, where the conditions are drier. Thus, the climate variability in R2 is socially more relevant, given people's dependence on the Grande River (see Figure 2.2) on this orographically-caused high rainfall center.

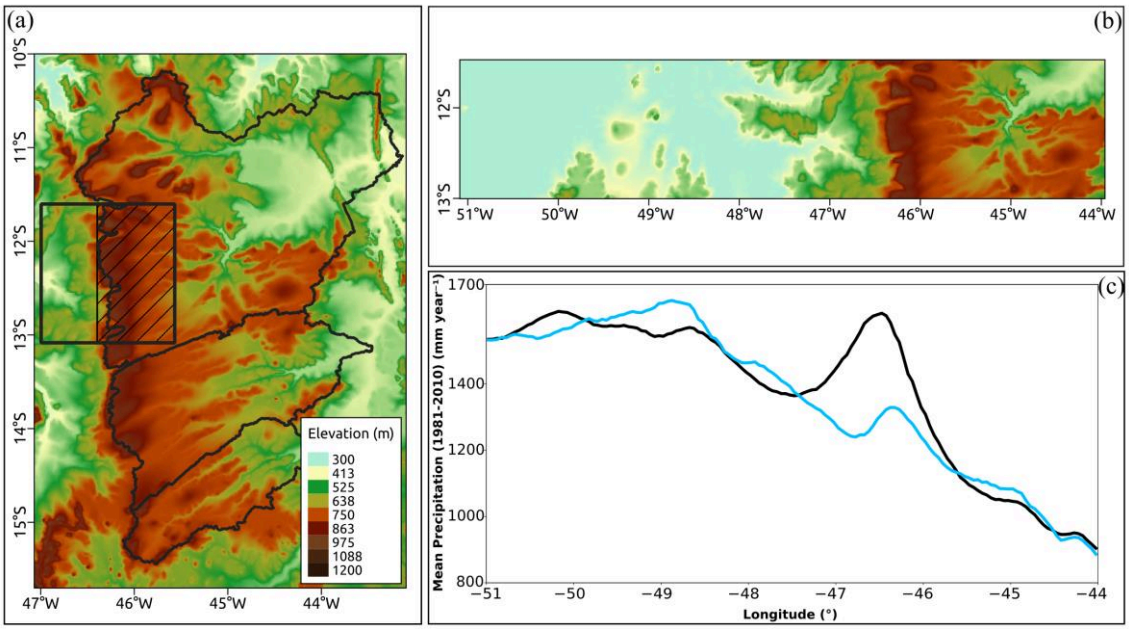

Figure 2. 3. (a) General view of topography for Western Bahia, and the steep transition to the west. The rectangle represents the two regions of interest, R1 and R2, as defined in Figure 2.2. (b) Broader view of the topography for the latitudes 11.5°S to 13°S. (c) Long-term mean precipitation (1981-2010) cross-sections for two latitude bands. The black line shows the cross-section of the mean precipitation for the latitudes 11.5°S to 13°S, and the light blue line shows the cross-section of the mean precipitation for latitudes 13°S to 14.5°S. Despite a general decreasing precipitation trend from west to east, the precipitation increase between 46°W and 47.5°W in the 11.5°-13°S range is caused by orography. R1 represents the region under the influence of orography. The western part of R1 drains to the west, where conditions are wetter, while R2 represents the subset of R1 that drains to the east, where the conditions are drier.

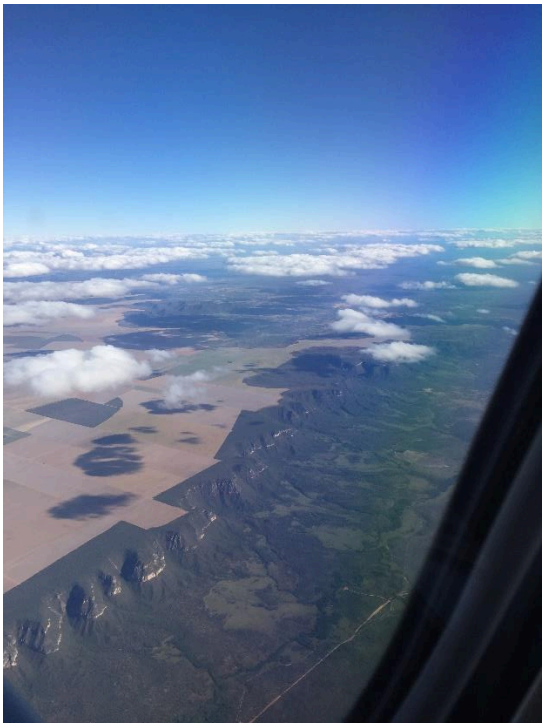

Figure 2. 4. An Aerial view shows to the left, the Chapada, and in the center, the Serra Geral de Goiás, a steep topography difference (> 300 m). Photo credit: Marcos Heil Costa.

The west-to-east, seasonal, and long-term rainfall variation directly impacts UAS recharge, and subsequently, river flows and water availability. Thus, the UAS and the flow of the draining rivers have an important role in the region's economic development.

Irrigation is an important practice in the region, increasing yields and doubling the crops planted yearly. Irrigated areas have increased over 1000% from 1990 to 2020 (Pimenta et al., 2021). The town of Luis Eduardo Magalhães (Figure 2.2), for example, was just a small village around a gas station in the 1980s, currently has around 90,000 inhabitants and has one of the highest agricultural GDP (Gross Domestic Product) per capita in Brazil. The increase in recent years has made the region also advance socioeconomically, and the irrigated area contributes 34% of the Gross Value of Agricultural Production (ABAPA, 2020). Agribusiness is responsible for 49% of the jobs in the region (AIBA, 2018), and, in 2017, there was an 84% increase in the generation of rural jobs compared to the previous year (AIBA, 2018). Although the increase of irrigated areas has significantly grown in the last 30 years, the total percentage of irrigation in Western Bahia is still considered small, just under 8% of total agricultural lands.

As the irrigation area increased, so did the water demand (Santos et al., 2020). However, intense irrigation growth is only part of the region's environmental problems. Pousa et al. (2019) analyzed time series of precipitation for 1980–2015 and river discharge for 1978–2015,

indicating a shift in precipitation patterns around 1992 ($p < 10^{-8}$), a significant reduction of up to 12% in rainfall since the 1980s ($\alpha = 0.05$) and a reduction in river discharge in all stations studied, in both the rainy season and the dry season. The combination of increased demand with a reduced supply of water resources has led to a series of water conflicts in the region in the last decade. A large part of the water use conflicts appears in the Grande and Corrente basins, mainly in the Rio de Janeiro sub-basin upstream of station B (Figure 2.2; Table 2.1). The reductions in precipitation were most significant in R1, where the precipitation is also higher, and the orographic effects are stronger. The main cause of a rainfall maximum in R1 – orography – obviously has not changed within this time frame. Although teleconnections triggered by large-scale processes like the warming of the tropical North Ocean may have contributed to a reduction in precipitation throughout northeast Brazil (Marengo et al., 2017), here we focus on the maximum reductions that happened in R1. We hypothesize that interactions between large-scale processes (SST) and mesoscale processes (orographic uplifting) define long-term rainfall variability in Western Bahia, particularly in R1. Since most croplands are located further west of the region, rainfed croplands are extremely sensitive to climate variability, while water resources availability and irrigated agriculture are extremely sensitive to long-term rainfall patterns.

This study aims to investigate how the interactions between large-scale features, regional topography, and groundwater influence the long-term variability in climate, water resources, and agriculture development in one of the most important producing regions.

2.2. Data and methods

2.2.1. Precipitation and river flow data

The regional patterns are characterized by the monthly precipitation dataset of CHIRPS (Climate Hazards group Infrared Precipitation with Stations v2 - https://data.chc.ucsb.edu/products/CHIRPS-2.0/). This data is available at a grid resolution of 0.05° x 0.05° (approximately 5 km x 5 km) for the 40 years of 1981-2020. CHIRPS derives gridded precipitation data from a combination of data sources, which includes: Climate Hazard Precipitation Climatology (CHPclim); infrared satellite observations; two atmospheric model precipitation fields, from Climate Forecast System (CFS) and National Oceanic and Atmospheric Administration (NOAA); the TRMM Multi-satellite Precipitation Analysis (TMPA); and precipitation observations from rainfall gauges (Funk et al., 2015).

Pousa et al. (2019) revealed a major shift ($p < 10^{-8}$) in precipitation time series in 1992 using the Pettitt's test and the 0.5° × 0.5° Xavier et al. (2015) precipitation database, which covers the period 1980-2015. Following this study, we divide the 40-year time series into two periods, namely P1 (1981-1992) and P2 (1993-2020), and use the Student's t-test to test the hypothesis of changes in mean precipitation between the two periods. The main difference between this analysis and the former Pousa et al. (2019) analysis is that this study analyzes these two periods with a higher resolution (0.05° × 0.05°) and longer (1981-2020) database from CHIRPS. The periods are also slightly different: Pousa et al. (2019) considered P1 = 1980-1992 and P2 = 1993-2015, while this study considers P1 = 1981-1992 and P2 = 1993-2020.

The daily river flow data (m^3/s) used are provided by the Brazilian Agency for Waters ANA (*Agência Nacional das Águas*). Some data has been available since the 1930s, but the few available stations had about 30% of gaps in the data series. After 1978, the quantity of fluviometric stations and quality of their data was increased, achieving only 2% of gaps. In this study, we used a time series from 1981 to 2020 for six fluviometric stations, the same used by Pousa et al. (2019) (Table 2.1). These stations are located throughout the region and represent regional variability. Stations A-D have dense irrigation systems upstream, while stations E-F have low irrigation density upstream (Figure 2.2; Table 2.1).

We applied the Kolmogorov-Smirnov test (KS) to detect changes in the river flow. KS is a nonparametric test of the equality of one-dimensional provability distributions. Here it is used to compare two samples (two sample K-S test) of a stream flow data in two periods (P1 and P2). We used the 2-sided KS test to evaluate the maximum distance (D, Equation 2.1) between two-sample distributions (Massey et al., 1951).

$$D_{P1,P2} = max(|F_{1,P1}(x) - F_{2,P2}(x)|) \quad (2.1)$$

where, $F_{1,P1}$e $F_{2,P2}$ are cumulative distribution functions of the P1 and P2, respectively. The test answers the question, “what is the provability that these two sets of samples were drawn from the same (but unknown) probability distribution?”.

In this study, we do not use the directly measured discharge Q but rather the "naturalized flows" series for each river at each station prepared by Santos et al. (2020). The naturalized flow (Q*) is the corresponding flow that would occur in a river section if there were no anthropic actions in the drainage area contributing to the section. The naturalized series are synthetic series created to reproduce the river's original flow through the return of the water used for irrigation back to the river, i.e., $Q^* = Q + Q_i$. More details on the procedure used to

calculate the irrigation flow Q_i and the naturalization process are available at Santos et al. (2020).

Table 2. 1. Selected river flow stations. The letters represent the station labels in Figure 2.1.

	ANA Station Code	River	Station Name	Municipality	Drainage Area (km^2)	Station Coordinates
A	46543000	Rio de Ondas	Fazenda Redenção	Barreiras	5383.758	12° 08´ S, 45°06´ W
B	46570000	Rio de Janeiro	Ponte Serafim	Barreiras	2522.118	11° 54´ S, 45° 36´ W
C	46415000	Rio Grande	Sítio Grande	São Desidério	4943.866	12° 25´ S, 45° 05´ W
D	45840000	Rio Formoso	Gatos	Jaborandi	7132.696	13° 42´ S, 44° 38´ W
E	45910001	Rio Corrente	Santa Maria da Vitória	Santana	29,643.66	13° 24´ S, 44° 12´ W
F	46790000	Rio Preto	Formosa do Rio Preto	Formosa do Rio Preto	14,326.87	11° 03´ S, 45° 12´ W

2.2.2. The Atlantic Multidecadal Oscillation (AMO)

To evaluate the possible influence of AMO variability with precipitation, we correlated the AMO index with the monthly precipitation average of the area. This index is a monthly series calculated from 1856 to the present (NOAA, 2001). It is obtained through the average of the detrended monthly SST (Sea Surface Temperature) anomalies in the North Atlantic Ocean (Enfield et al., 2001).

To investigate potential teleconnections between the AMO and the regional precipitation patterns, we perform a lag correlation analysis between the sum of precipitation of the December and January months and the AMO monthly index calculated for the period 1981-2020 (lag = -12 to 0 months).

2.2.3. Climate Reanalysis data (ERA5)

The ERA5 reanalysis from the ECMWF (European Centre for Medium-Range Weather Forecasts), with a horizontal resolution of 0.25° x 0.25°, was used to characterize the circulation associated with wettest and driest years. We used wind speed and geopotential height for this characterization at 16 pressure levels between 1000 hPa and 500 hPa. To better compare with topography, all fields were interpolated from the original 16 pressure levels to 23 height levels using log-linear interpolation. We used the omega for zonal vertical velocity analysis. For the zonal precipitation analysis, in addition to the CHIRPS data, we also use the ERA5-Land rainfall data, with a resolution of 0.1° x 0.1°. As explained in Section 2.3.3, we considered the sum of bimester December and January (DJ) in Region 2 (Figure 2.3b) and selected the five rainiest and the five driest bimesters between 1981 and 2020.

To calculate the approximate pressure (p) levels at each height, we used Equation 2.2, based on the International Standard Atmosphere:

$$p = p_0 \left(1 - 0.0065 \frac{h}{T_0}\right)^{5.2561} \quad (2.2)$$

p_0 is the sea level pressure (1013.25 hPa), h is the altitude, and we assumed T_0 = 25°C, the mean average air temperature for the region.

2.3. Results

Results from Sections 2.3.1 and 2.3.2 are essentially a confirmation of Pousa et al.'s (2019) results using a longer time series. The new results of this study are presented in Sections 2.3.3 and 2.3.4.

2.3.1. Precipitation changes

Figure 2.5 shows the regional mean precipitation for the two periods (P1 and P2). The isohyets have moved westward from P1 to P2 (Figure 2.5a,b), exhibiting a regional drying of P2 related to P1 in all three basins (Figure 2.5c), except in the north and east parts of the Grande river basin. Although the decrease in precipitation is widespread in the southwest of the Grande, and throughout the Corrente and Carinhanha river basin, mainly in Regions 1 and 2 (R1 and R2) show a significant reduction in precipitation ($\alpha = 0.05$). Region 1 rainfall decreased by -176 mm year^{-1}, in P2, compared to the P1 mean, while Region 2 rainfall decreased by -170 mm year^{-1}, approximately 11.5% for both regions. These two regions are surrounded by very likely ($\alpha = 0.10$) reductions in precipitation (Figure 2.5c).

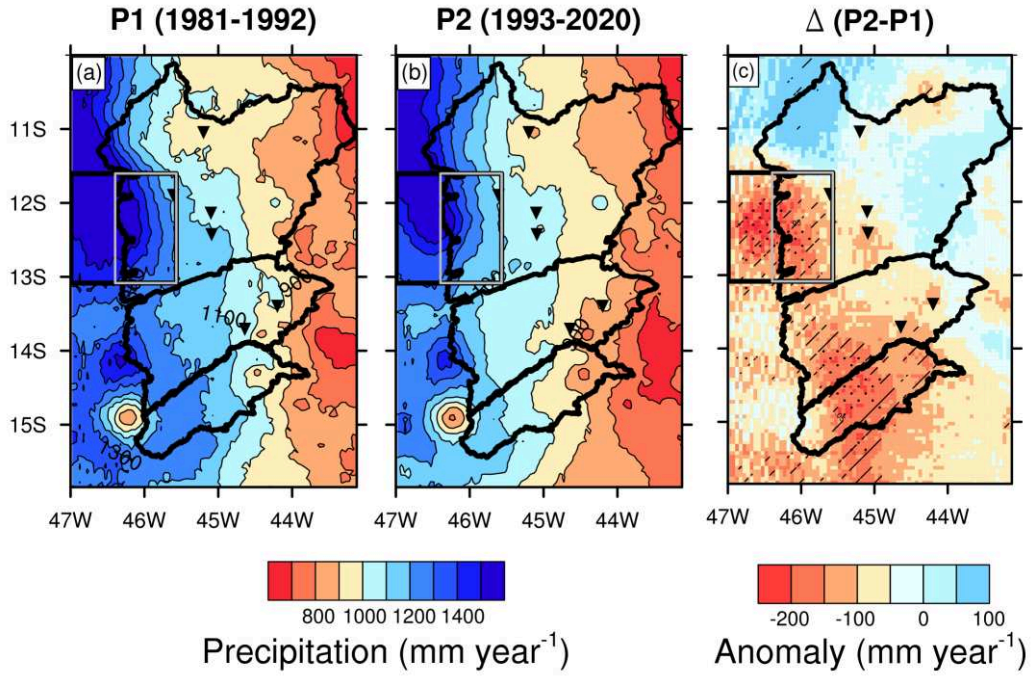

Figure 2. 5. Average precipitation map for periods P1 (**a**), P2 (**b**), the difference between P2 and P1 (**c**). The rectangles are Regions 1 and 2, and the triangles mark the locations of river flow stations shown in Table 2.1. Dotted areas represent differences significant at $\alpha = 0.05$, according to Student's t-test (in c), while shaded areas represent differences significant at $\alpha = 0.10$.

2.3.2. River flow changes

The cumulative probability in Figure 2.6 shows the six stations analyzed in this work (Table 1). The curves represent the probability of specified discharge occurring in each period. For all stations, the discharges P2 are considerably less than P1, mainly in the minimum's discharges, where the Q_{90} are defined.

To further evaluate the statistical difference, the KS test and the p-value show highly significant differences in all six stations, inferring that sample P2 is significantly different from the sample P1 (Figure 2.6). For all stations $p < 10^{-5}$, except for station B, where $p = 0.022$.

Q^*_{90} is the flow expected to be present in the river at least 90% of the time, i.e., during 90% of the time series used in the calculation, there is a flow equal to or greater than Q^*_{90} in the river. The State of Bahia grants water use permits in the Grande and Corrente basins using the criterion that 80% of Q*90 can be granted for human use (Pousa et al., 2019). Table 2.2 shows the evolution of Q^*_{90} calculated in three different periods for stations A-F.

Table 2. 2. Rate of change of the naturalized discharge with 90% permanence (Q^*_{90}) with time.

ID	ANA Station Code	Q^*_{90} (m^3/s)			Rate of change ΔQ^*_{90}/decade	
		1978-2000	1978-2010	1978-2020	(m^3/s/10 yrs)	(%/10 yrs)
A	46543000	38.95	35.66	30.43	-4.26	-10.9%
B	46570000	8.78	8.36	7.64	-0.57	-6.5%
C	46415000	25.9	22.23	19.96	-2.97	-11.5%
D	45840000	64.96	60.88	54.22	-5.37	-8.3%
E	45910001	169.40	150.90	144.17	-12.62	-7.4%

There has been clear drop in Q^*_{90} flows over the last 20 years, even considering the naturalization of the flow, that is, even returning the water withdrawn for irrigation to the rivers. Q^*_{90} has dropped from -11.5% per decade in Rio Grande to -6.5% per decade in Rio de Janeiro. These trends (and their spatial variations) are justified by precipitation reduction in the region, as discussed in Section 2.3.1.

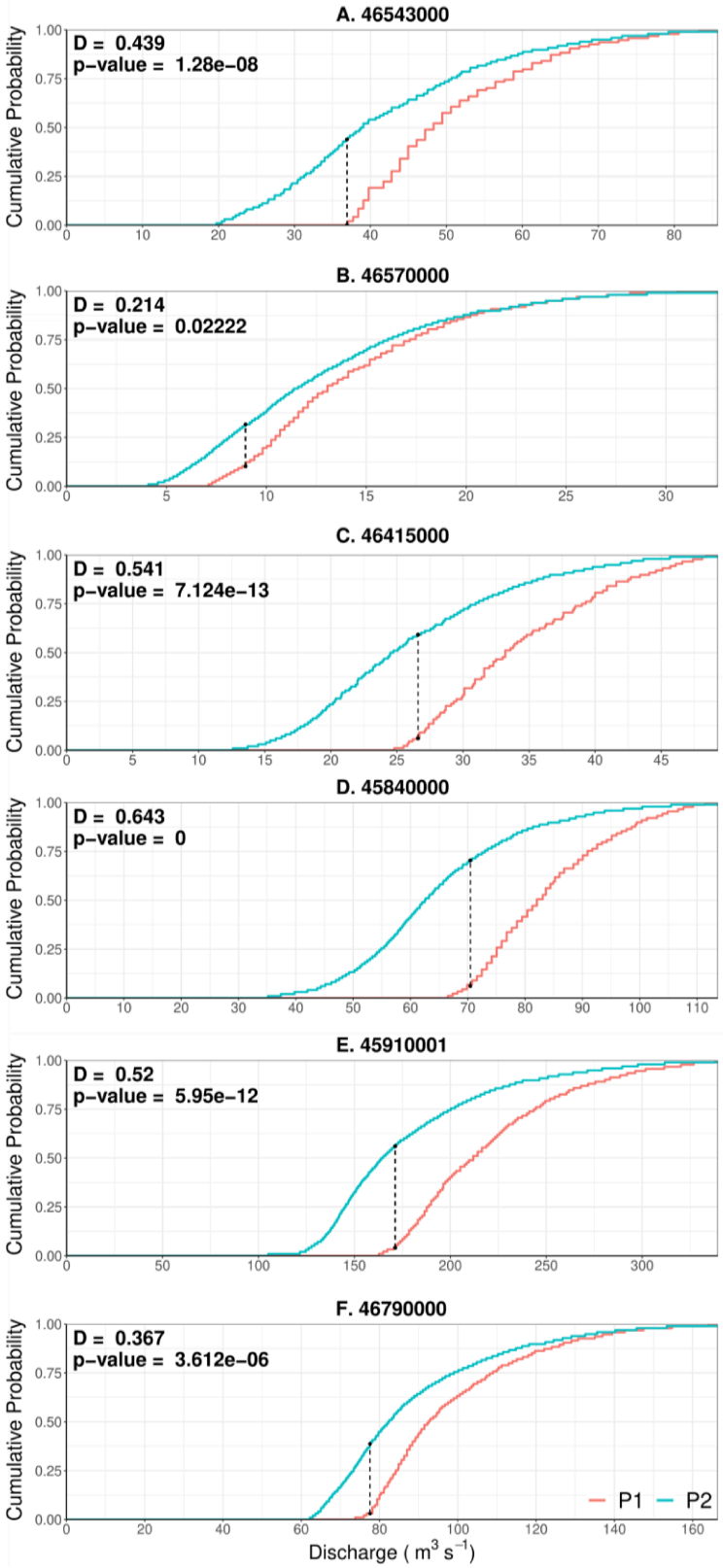

Figure 2. 6. Cumulative probability of the discharge data in six stations (A-F), also showing KS (D) statistic between P1 and P2.

2.3.3. Correlation of monthly regional precipitations with AMO

The AMO was in its cold (negative) phase from 1981 to the early 1990s, shifting to the warm (positive) phase around 1994-1995, depending on whether the monthly or 12-month running means are used (figure 2.7a). The shifting patterns in AMO coincide with the changes in precipitation and river discharge observed in Figures 2.5 and 2.6.

Figure 2.7b shows that the rainfall differences between from P1 and P2 in Region 2 are only statistically significant ($\alpha = 0.05$) in the two months of higher precipitation in P1 (December and January). Our interpretation is that the long-term changes in the mean precipitation shown in Figure 2.5 result from the reduction in precipitation in these two rainiest months. Therefore, we analyze the sum of precipitation for the bimester of December and January (DJ) from now on.

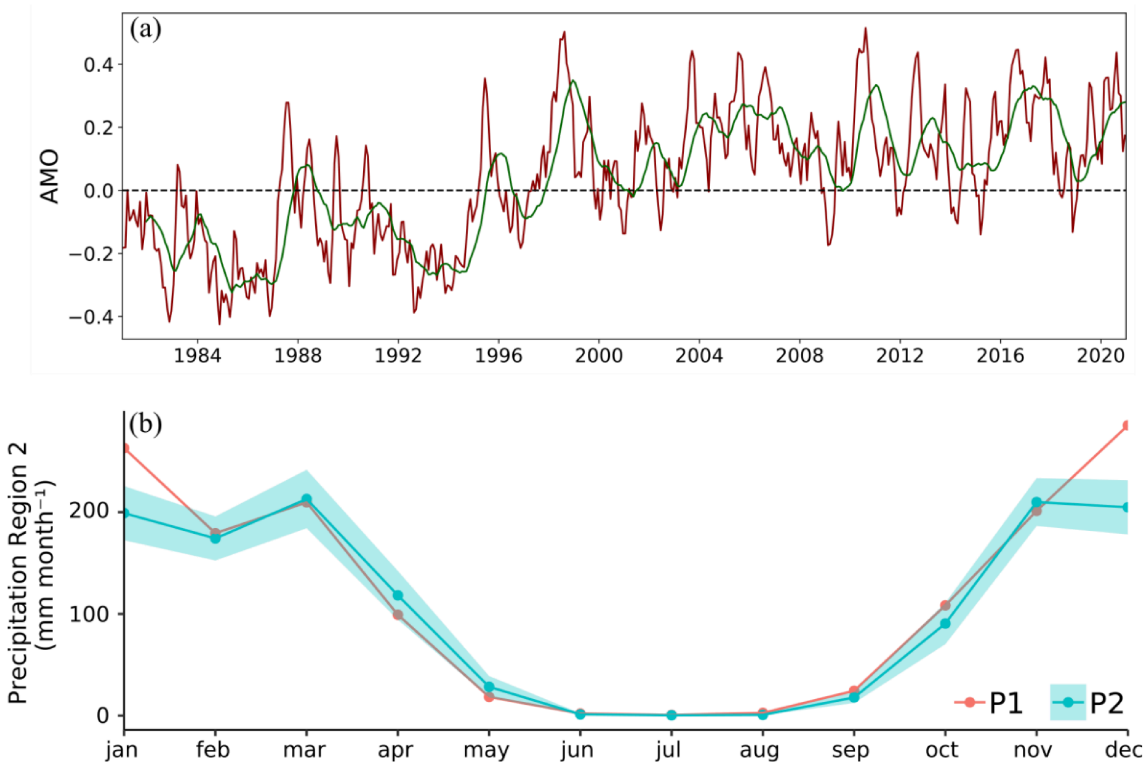

Figure 2. 7. (a) the evolution of the monthly AMO index in salmon and the 12-month moving average in green. (b) the average monthly precipitation for Region 2 divided into periods P1 (1981-1992) and P2 (1993-2020). The shaded area in P2 is the confidence interval for the mean ($\alpha = 0.05$). Averages in P1 outside the shaded area are statistically different at this confidence level.

A lag correlation was performed for the sum of DJ precipitation (Figure 2.8) with the monthly AMO index (except for the lag 0, which was performed with the average AMO index for December and January). Highly significant correlations (p-value ≤ 0.01, red dots) indicate a potential teleconnection of dynamic circulation patterns driven by the AMO with the DJ

precipitation in Regions 1 and 2. In Region 2 (Figure 2.8b), the correlations are stronger, showing statistical significance (p-value ≤ 0.01) for every lag correlation from zero to -12 months. The correlation values are higher than -0.6 for 0 and 1-month lags, reaching a maximum of -0.62 for 1-month lag (November AMO). For Region 1 (the larger region, which includes Region 2 – Figure 2.8a), correlations are not as high, with the most significant correlation (p-value ≤ 0.01) for 0, 2 and 3-months lags, reaching the highest negative correlation with September AMO (lag = -3, R = -0.44). However, the lag correlations were significant at $\alpha = 0.05$ for most month-lags from 0 to 12. In addition, I evaluated rainfall data from the Correntina station (see location in Figure 2.2), which spans a longer period, 1961 to 2020. The correlations are similar to the ones of Regions 1 and 2, with a significant lag correlation for 0-month (R = -0.41, p-value ≤ 0.01) and -1 to -3 months (p-value ≤ 0.05). The negative correlation implies that the DJ precipitation decreases when the AMO index is higher.

We also evaluated the correlations between DJ and PDO (Pacific Decadal Oscillation) and ENSO (El Niño Southern Oscillation), but there was no significant correlation.

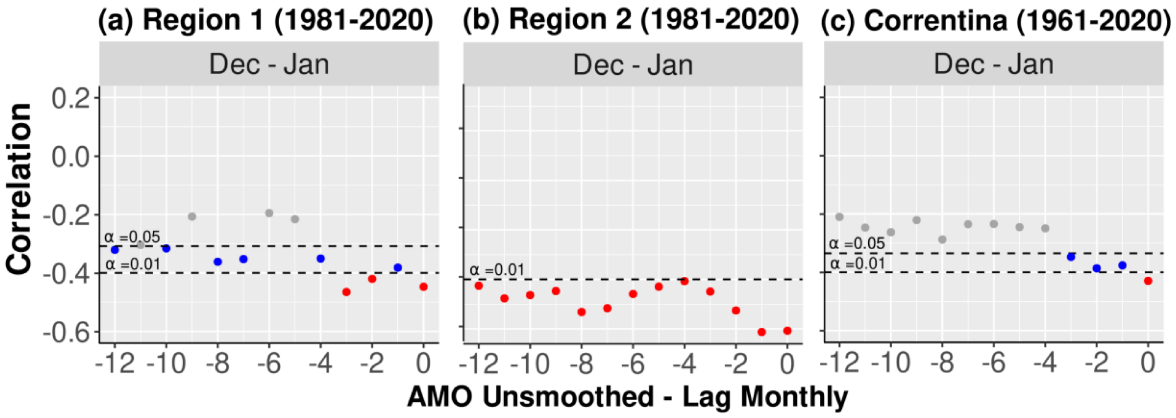

Figure 2. 8. Lag correlation between monthly AMO and DJ precipitation. The red points represent a statistically significant correlation (p-value $\leq$ 0.01), and the blue points (p-value ≤ 0.05). The gray points represent a statistically non-significant correlation (p-value > 0.05).

2.3.4 Dynamics of the interaction between large-scale and mesoscale processes

The fact that the precipitation in the region under the influence of orography (R1) also correlates with AMO indicates a possible interaction between large-scale processes (AMO) and mesoscale processes (orography). Moreover, the higher and more persistent lag correlation in R2 suggests different climate mechanisms in the west and east of the Serra Geral de Goiás.

To evaluate these interactions, first, we selected the five rainiest and driest DJ bimesters in the time series (Table 2.3). Not surprisingly, all five rainiest bimesters occurred before 1992 (1984/85, 1985/86, 1987/88, 1989/90, and 1991/92). Similarly, all five driest bimesters occurred after 1993 (1994/95, 2007/08, 2012/13, 2016/17, and 2017/18).

Table 2. 3. Five rainiest and five driest DJ bimesters in the period 1981-2020.

Rainiest		Driest	
Year	Amount (mm)	Year	Amount (mm)
1984/85	684.88	2016/17	258.49
1989/90	650.58	2017/18	332.90
1987/88	630.97	2007/08	334.76
1991/92	603.76	2012/13	345.96
1985/86	598.35	1994/95	359.33

The sea surface temperature (SST) of the North Atlantic seems to have a significant modulation of DJ precipitation variability. Figure 2.9 shows the DJ precipitation and wind circulation in a transect (longitude versus altitude/pressure) averaged over the 11.5°S and 13°S band of latitude for the five rainiest and driest DJ bimesters, along with the details of topography, and other geographical features.

For the average wettest bimesters (Figure 2.9a), the wind comes from both west and east, converging between 46°W and 50°W. Ascension of the easterly winds is modulated by orography. At the same time, the westerlies start to ascend a few hundred kilometers before the Serra Geral de Goiás (limit between Tocantins and Bahia), probably due to the low-level convergence. Strong vertical winds, resulting from both orography and convergence, cause high rain rates throughout the cross-section, with maximum values bigger than 600 mm (in two months) from 51°W to 46.4°W, decreasing to the east in Bahia, but still reaching values as high as 500 mm around 44°W. The ascension of wind is more intense above 2000 meters and shows no sign of divergence at 5000 meters, indicating no inhibitions for deep convection.

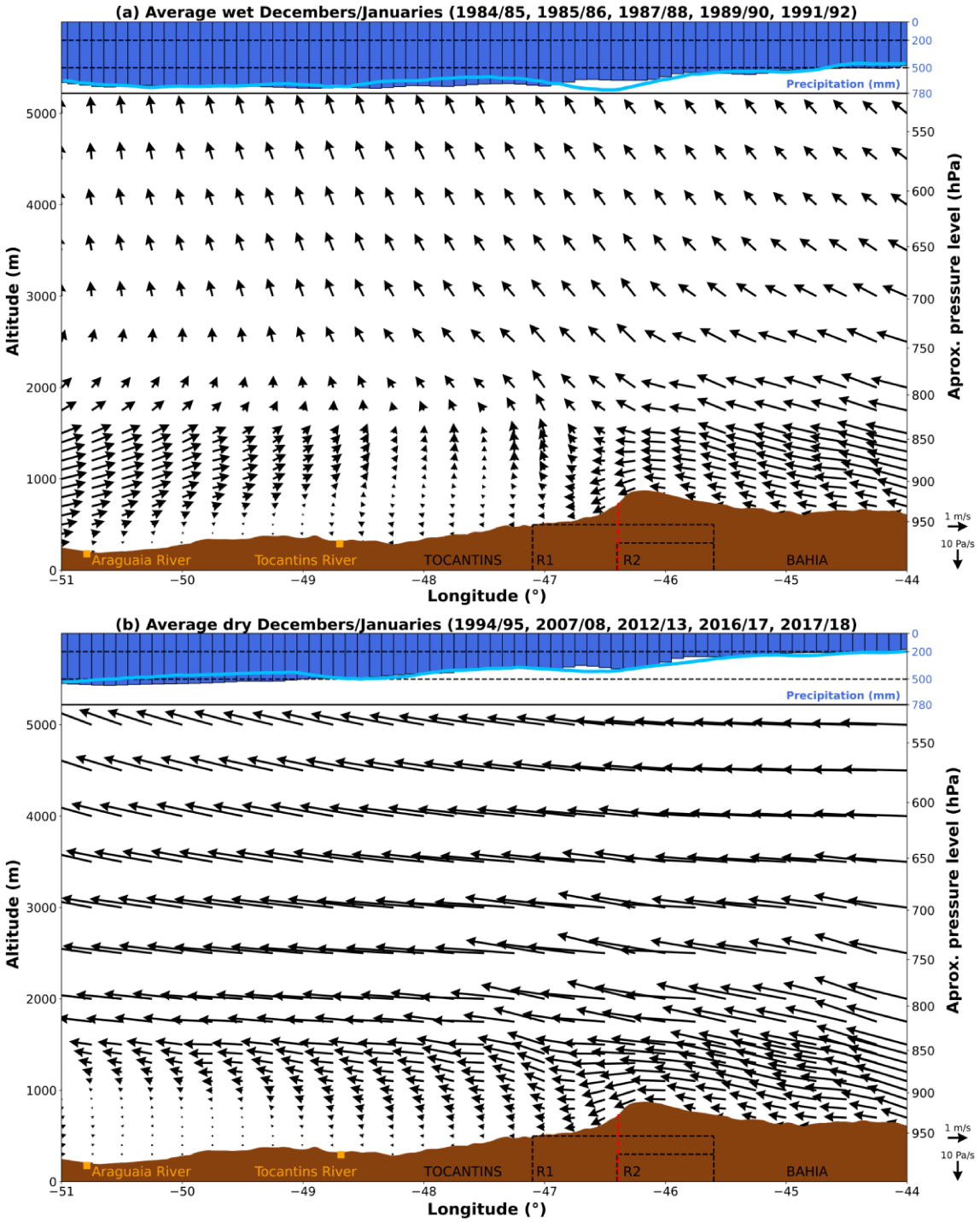

Figure 2. 9. Atmospheric circulation averaged between latitudes 11.5ºS and 13ºS for the wet bimesters (a) and the dry bimesters (b). Arrows represent zonal and vertical wind velocities. Surface elevation is shown in brown. Blue vertical bars at the top show each latitude's ERA-5 average precipitation in those months, while the light blue line is the average precipitation by CHIRPS. Approximate pressure levels at the right vertical axis were calculated based on the international standard atmosphere (Equation 1). The figure also shows R1 and R2, the division of Bahia and Tocantins (red line), and the Araguaia and Tocantins rivers (also seen in Figure 2.1).

The picture is completely different for the five driest bimesters (Figure 2.9b). First, there is no convergence of easterlies and westerlies, with easterly winds dominating the transect. Easterlies get a slight vertical acceleration from orography between -44°W and -46.5°W, but the resulting convection in the R1 domain is shallow and suppressed between 3 and 4 km of altitude. The westerly winds from the Tocantins, which bring moisture from the Amazon region, are blocked and do not enter this transect. The resulting precipitation gradient is a much steeper one. Precipitation in the Tocantins state is reduced between 10% and 25%, reaching between 520 mm to 450 mm from -51°W to -46.4°W. It then decreases steeply, reaching only 200 mm at -44°W, a value 60% below that of the rainiest bimesters.

The far-reaching easterlies in the driest years indicate that the subtropical high still predominates in this region in DJ. Moreover, the easterly winds carry dry air from Caatinga in Northeast Brazil. In contrast, the subtropical high has already receded in DJ in the rainiest years, allowing for a strong convergence along the transect.

Focusing only on Region 1 and Region 2 (R1 and R2) in Figure 2.9, one can observe that the Serra Geral de Goiás contributes to the east-west variation in the precipitation regime. It rains more in the western portion of R1 than in the eastern portion (the same as R2).

The western portion of R1 drains to the Tocantins river basin, where the annual mean rainfall is ~1600 mm yr^{-1}. On the other hand, the rain over R2 will recharge the Urucuia aquifer and contribute to the river discharge that flows east, being an important source of water draining into Brazil's semi-arid region.

2.4. Discussion

2.4.1. The large-scale influence on regional precipitation

We investigated the changes in atmospheric patterns and how the large-scale interaction can influence regional precipitation. In the last years, extreme drought events have been associated with the ENSO and the northward position of the intertropical convergence zone (ITCZ) (Marengo et al., 2017). However, these events controlled the interannual variability, associating El Niño events with negative precipitation anomalies in NEB and La Niña events with positive precipitation anomalies (Marengo et al., 2017). Nonetheless, the AMO, a low-frequency, multidecadal variability mode, marked the long-term changes in precipitation in Western Bahia. Figure 2.7a shows a change from a negative to a positive phase around 1993 in the AMO series.

I associate this year with the changing point (1992 to 1993) in the precipitation series detected by Pousa et al. (2019). Our results show a statistically significant correlation between monthly precipitation and the 12-month lags for Region 2, which means decreasing precipitation when the AMO index is positive. Previous studies showed a connection between anomalous Walker cells and Atlantic Hadley cells with the influence of the AMO and the rainfall variability in NEB (Kayano et al., 2016, 2017; Shimizu et al., 2021). In a recent study, Shimizu et al. (2021) analyzed the Walker and Hadley cells changes between two periods of AMO, cold (1981-1997) and warm (2002-2019). These periods are almost the same as our P1 and P2. Their results show that the ascending branch of the Walker circulation migrated from the east (40°-50°W) to the west (60°-70°W), producing anomalous subsidence over the region 40°-50°W; 0°-10°S). Based on these results, we further investigated the atmospheric dynamics extending the latitudes, including Western Bahia (0°-16°S). First, we analyzed the mean vertical velocity at 500 hPa, a non-diverging level of the atmosphere. The positive anomaly of the periods (P2-P1, Figure 2.10c) indicates increased subsidence, inhibiting upward vertical movement.

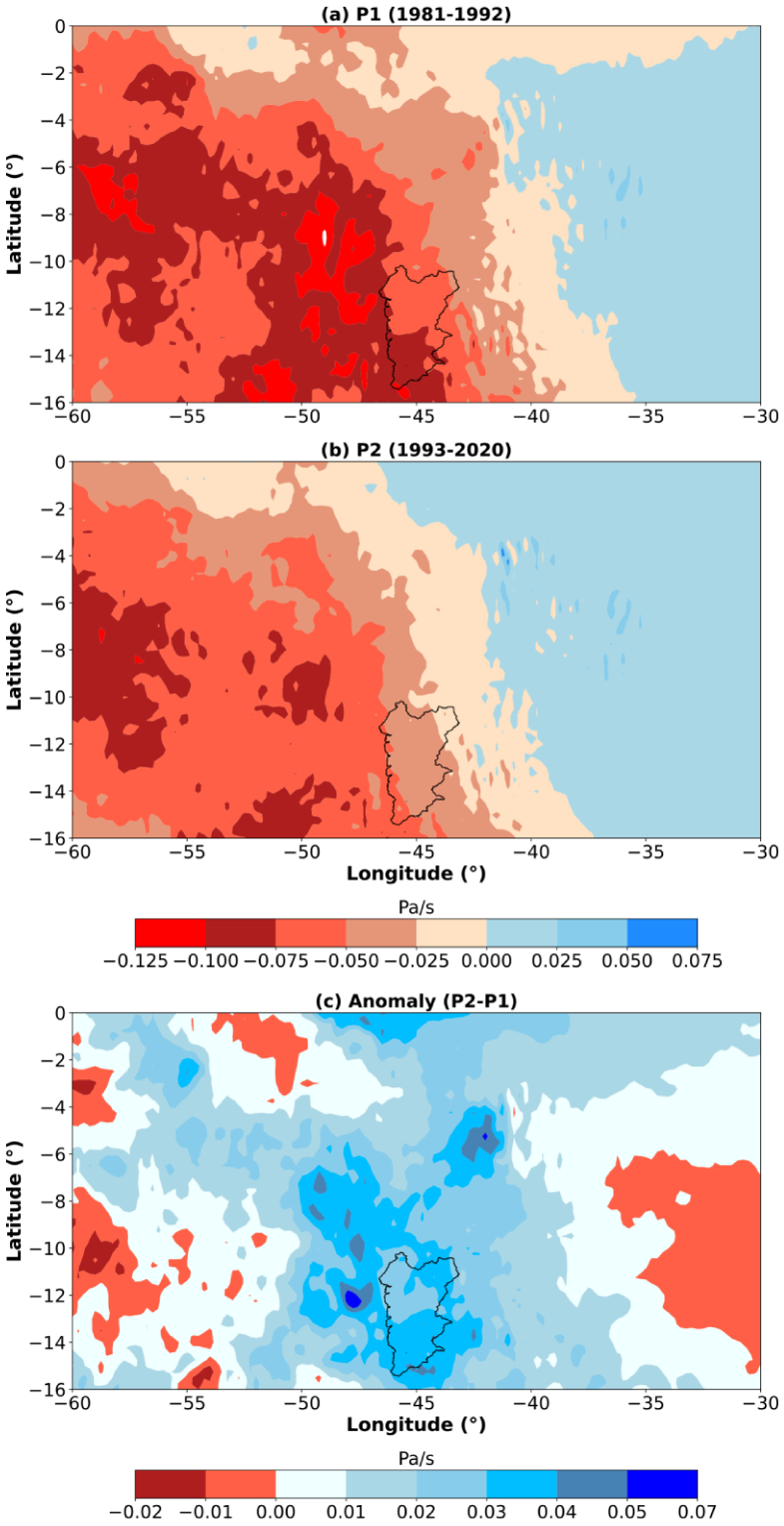

Figure 2. 10. Mean vertical velocity (Pa/s) at 500 Pa for 0°-16°S for periods P1 and P2 in bimester DJ: (a) P1 (1981-1992) and (b) P2 (1993-2020). Negative values indicate upward motion, and positive values indicate downward motion. (c) the difference between the two periods. Positive values indicate increased subsidence

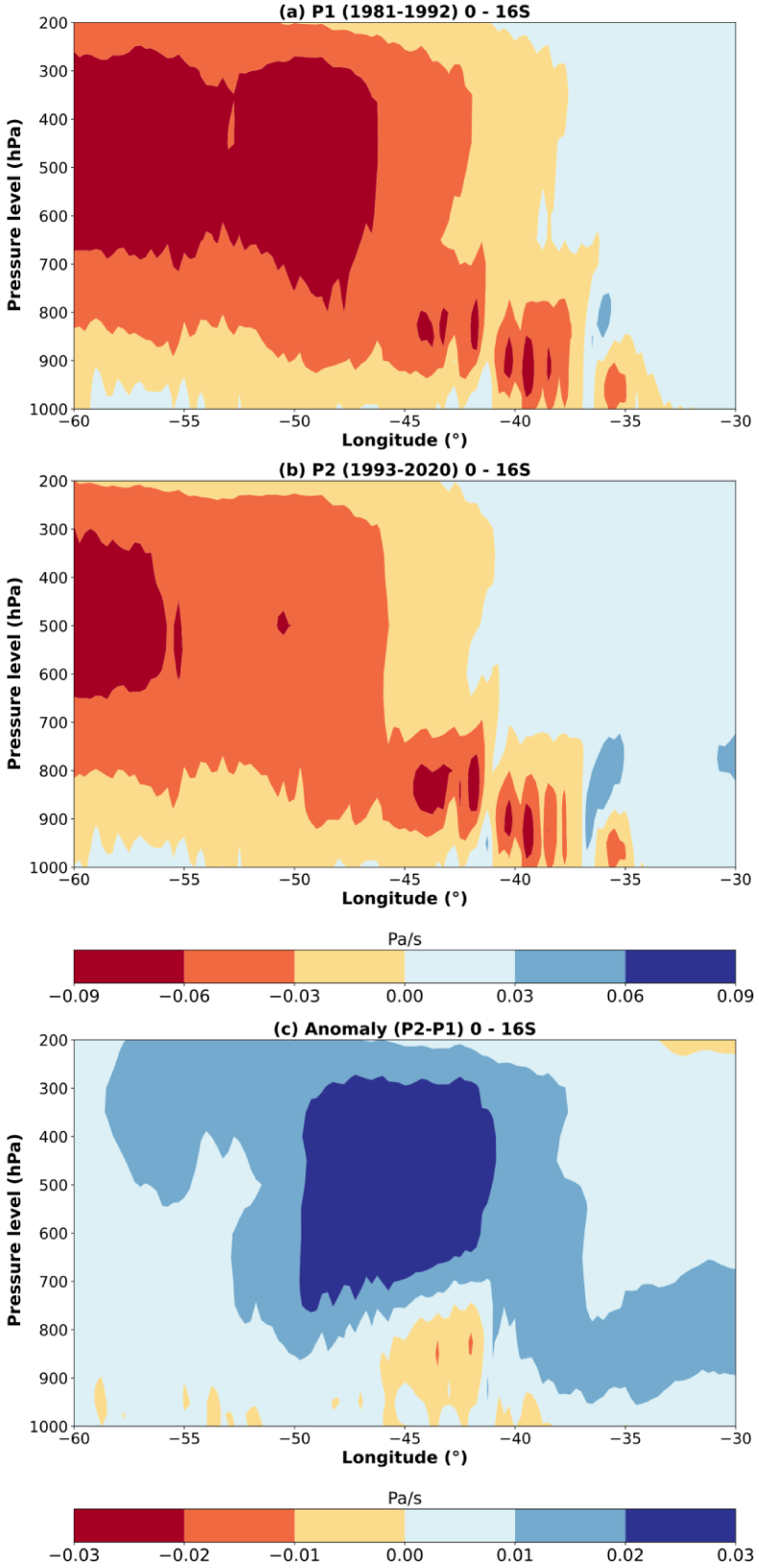

Figure 2. 11. Meridional mean (0°-16°S) cross-section of the vertical velocity (Pa/s) for periods P1 and P2 in the bimester DJ: (a) P1 (1981-1992) and (b) P2 (1993-2020). Negative values indicate upward motion, and positive values indicate downward motion. (c) the difference between two periods. Positive values indicate increased subsidence.

Figure 2.11 is a cross-section analysis similar to the one shown by Shimizu et al. (2021) but extending to 16 °S and restricted to DJ only. Considering two periods P1 and P2, I analyzed the changes between the Walker and Hadley cells and AMO phases. The downward branch of these cells shifted from east to west (Figure 2.11 a,b). There is increased shallow convection (bellow 750 hPa) in the range 42°W to 46°W, but a major subsidence anomaly above 750 hPa. This patter inhibits deep convection in the two rainiest months of the year, considerably reducing the total amount precipitated in this bimester. The subsidence anomalies in Figure 2.11c (positive values) inhibit the formation of deep clouds resulting in a decrease in precipitation. These results (Figure 2.11), are consistent with detailed analysis in Figure 2.9, where a rainfall reduction is shown from west to east.

2.4.2. Climate variability increases zonal climate gradient

If considered individually, the Tocantins-Araguaia River Basin is the third largest river basin in Brazil, after the transnational Amazon and the Paraná-La Plata systems. It is also the largest river basin entirely in Brazil, with a drainage area of 803,000 km² and a long-term mean discharge of 13,600 m^3/s at the mouth (17 L s^{-1} km^{-2}). To the east, the São Francisco River Basin is the fourth largest river basin in Brazil, and the second-largest river basin entirely in Brazil, with a drainage area of 641,000 km² and a long-term mean discharge of 2,800 m^3/s at the mouth (4.4 L s^{-1} km^{-2}). Despite their similar size, the Tocantins-Araguaia system has a much higher discharge because it drains a much rainier region. In contrast, the São Francisco drains a basin that is, in part, semi-arid. The rivers that drain the Urucuia aquifer contribute 881 m^3/s, about one-third of the total annual flow of the São Francisco River at Barra (2620 m^3/s – Vieira et al., 2021), where the Grande River discharges into the São Francisco (Figure 2.2).

Considering the cross-section analyzed in Figure 2.9, we can point to a transition of the Cerrado biome to the west and the semi-arid Caatinga biome to the east. To the west of this cross-section (51°W) the annual precipitation is > 1900 mm $year^{-1}$, contributing to two important rivers in the state, Araguaia and Tocantins rivers. On the border with the Bahia state, specifically in the Serra Geral de Goiás, the annual precipitation is ~1200 mm $year^{-1}$, and in the eastern baoundary of the cross-section (44°W) the long-term precipitation climatology is < 800 mm $year^{-1}$ (Alvares et al., 2014; Pousa et al., 2019).

This work suggests that the rainfall difference between these two neighboring rivers may increase with climate variability. In the transect analyzed, the difference in the rainfall between

the rainiest and the driest years is 10%-25% on the Tocantins side, while it may reach 60% on the Bahia side.

2.4.3. The decreasing aquifer and river flows

To the west of 46.4 °W (State of Tocantins), rivers run to the west to contribute to the large Tocantins-Araguaia Basin. In this longitude range, rainfall is not much affected. On the contrary, to the east of 46.4°W, rainfall recharges the Urucuia aquifer, and rivers run east. As discussed earlier, Region 2, where rainfall is climatologically highest (Figure 2.1), has also been the most affected by reductions in rainfall (Figure 2.5).

This study updates Pousa et al.'s (2019) results for precipitation and river flow reductions. Pousa et al. (2019) have used direct rainfall and discharge measurements until 2015, and discharge measurements were not corrected by irrigation withdrawal. Here, we have included (i) rainfall and discharge data until 2020; (ii) expansion of the irrigated areas until 2020 (Pimenta et al. 2021); (iii) and used the naturalized discharge by adding the water withdrawal for irrigation to the river discharge until 2020 (Santos et al. 2020). As irrigation expands, the naturalization procedure adds more water to the direct discharge measurements.

Our results also suggest that the decline in water availability results from long-term climate variability. The reduction in rainfall directly impacts the aquifer recharge and aquifer levels. Marques et al. (2020) showed a decrease in aquifer levels in Alto Grande Basin reached over six meters from 2011 to 2018. This decay is directly connected with the decrease in rainfall and increase in irrigated croplands that use groundwater. The large Urucuia aquifer buffers rainfall variability into a less noticeable fluctuation in river flow decrease. Still, Region 2 is the main headwaters of the Grande river. Thus, the significant decrease in precipitation leads to discharge decreases mainly for stations A, B, and C (Figure 2.2; Table 2.1). However, precipitation reductions are widespread in Western Bahia, with different significant levels. Essentially, every river gauge shows a reduction in discharge (Figure 2.6), even when the discharge measurements are corrected by water withdrawal. The continued decrease despite the correction dismisses irrigation water use as the main cause of decreases in river discharge in Western Bahia.

Silva et al. (2021) analyzed the impact of land-use change and precipitation decrease on the water resources in the Pratudão River. The Pratudão is the northern tributary of the Formoso River, a sub-basin of the Corrente (Figure 2.2). They acknowledge the reduction in discharge in the Formoso (station D – 45840000) but argue that the significant precipitation changes

($\alpha = 0.05$) in Pousa et al. (2019) happened in just a small area of the headwaters in this sub-basin, and thus concluded that water appropriation by irrigation was the main reason for discharge reduction. Indeed, there was a major increase in irrigated areas upstream of station D, from 884 ha in 1990 to 33,887 ha in 2020 (Pimenta et al., 2021). We counterargue that, even after restoring the pumped water for irrigation upstream to 45840000, there is still a significant decrease in discharge. In addition, in this study, the area with a statistically significant reduction in rainfall is larger in the upstream Formoso due to a higher resolution dataset (Figure 2.2, Figure 2.5c). Moreover, statistically significant or not, there was a widespread decrease in rainfall across the sub-basin (Figure 2.5c). Given these persuasive arguments, we understand that the reduced rainfall in the region is the main reason why discharge has decreased on the Formoso sub-basin.

On the other hand, although the decrease in rainfall in the DJ bimester is far from the season when the minimum discharge occurs, this reduction will affect the aquifer recharge and the river discharge in the following months and years, and consequently, the grant flows (Table 2.2).

2.5. Conclusions

In Western Bahia, the expansion of irrigated areas has increased water stress. However, rainfall variability in the region is also a major driver that may lead to possible conflicts over water use.

The rainfall in the two rainiest months (December-January) is negatively correlated with the AMO index, indicating the warming of the North Atlantic sea surface temperature influenced the precipitation regime in Western Bahia. Moreover, an interaction between this large-scale climate process and a mesoscale process (orographically-induced precipitation) causes the greatest rainfall changes in the region where the maximum rainfall is.

This region of maximum precipitation has historically been important to support rainfed agriculture, recharge the Urucuia Aquifer System, provide water development for irrigation in the region, and contribute to about one-third of the water of the São Francisco river at the Barra station. This warm phase of the AMO has lasted for about 25-27 years. Although Enfield et al. (2010) have suggested that the current warm regime is expected to peak around 2020 and persist possibly as late as 2035, multidecadal climate predictions are still much uncertain to drive policies (Yang et al., 2021; Liu et al., 2021).

The climate variability in Wester Bahia is complex. In some years, the rainfall total is typical a semiarid climate, whereas in the other years, the rainfall total is typical of the Cerrado climate.

This complexity raises the hypothesis that this variability may not be linked only to the climate of NEB. Other large-scale mechanisms, such as the South Atlantic Convergence Zona (SACZ) and the South American Monsoon System (SAMS), may influence the regional rainfall regime and its interannual variability. The influence of these climate systems on the dynamics of the east-west transition in the Western Bahia region should be investigated in future works.

These large-scale mechanisms have been affecting the lives of the population in recent years. Especially in Region 2, where the rainfall essentially contributes to the Rio Grande Basin, with the rainfall decrease, the entire water supply to the region will be compromised, affecting water and food security. The region is very dependent on water resources and its economic and social development has been highly associated with rainfed agriculture and the expansion of irrigation. Since this basin has the highest agriculture output in Western Bahia, the effects on the economy may be considerable. In this context, the interaction of the North Atlantic Ocean and the local region has important consequences for the population in the region.

The possible maintenance of warmer than normal temperatures in the North Atlantic, either by natural variability or by anthropogenic drivers, will add increasing pressure on the water system of Western Bahia and all the economic activities that depend on them.

General Conclusions

In the last 40 years, Western Bahia has undergone an extensification of agriculture, mainly rainfed agriculture, and increase in irrigated agriculture. Irrigation has become an alternative for increasing yields and outputs. This thesis analyzed the regional hydroclimatic over the past 40 years, to help improve the water resources management of the region.

In Chapter 1, I analyzed long-term time series of precipitation and river discharge, comprising a period of 35 years, to evaluate the availability of water resources for irrigation. I considered the intense growth of irrigated areas in this period and interviewed irrigators to evaluate the demand and water resources. This study led to some conclusions. The irrigated area has increased since the 1990s, and by 90% in just eight years, 201-2018. Even considering this relatively short time series, the river discharge time series has proven non-stationary, which may be explained by the precipitation reduction in this period. Low-frequency climate variability and anthropogenic effects can influence the atmospheric circulation patterns that modify the time series of this variable. Thus, with reduced water availability and increased demand for water resources, Western Bahia potentially has seven areas with a critical situation of water use conflicts.

In Chapter 2, first, I used a longer time-series of precipitation and river discharge to confirm Chapter 1 results. Second, I investigated how the interactions between large-scale and mesoscale processes influence the long-term variability in climate and water resources, impacting agriculture development. This study led to some conclusions. The rainfall variability in Western Bahia is a major driver that may lead to possible conflicts over water use. In this chapter, I used finer resolution precipitation data and an extended river discharge for the 1981-2020 period that confirmed precipitation decrease already indicated in the first chapter. Also, I have shown that a teleconnection between a large-scale climate process (Atlantic Multidecadal Oscillation - AMO) and a mesoscale process (orography) leads to the highest rainfall changes in the precipitation series. In other words, when the AMO index is positive, indicating the warming of the North Atlantic sea surface, precipitation in Western Bahia decreases.

This thesis fills a gap in studies on which variables (the decrease in rainfall or the expressive use of water for irrigation) are most influential in reducing discharges in a region with high agricultural growth in recent decades. I showed that even with a correction in the discharges by returning water withdrawals to the river, the decrease in rainfall is the main cause influencing the hydrological regime in the region. This depletion is connected with the warming

of the North Atlantic Ocean. The strong convergence and strong orographic uplift in cold North Atlantic periods are not observed in warm North Atlantic conditions, when the orographic uplifting is suppressed.

This thesis analyzed all aspects of the water in the region, atmospheric, surface and underground. The high growth of irrigated areas and the decrease in rainfall align with the nexus context, the water-energy-food link (Hoff, 2011). Energy has its relevance in providing power for agricultural production and the whole society. And finally, the production of food, as a product present in the region not only for social but mainly economic sustenance. The approach of these three paradigms in this thesis shows that their integration and governance at different scales are extremely important for a strategic economic sector, agriculture.

This thesis shows the interconnection between these themes. For example, how the North Atlantic temperature influences the precipitation regime of important food production in NEB or how the soil-vegetation-atmosphere is connected to the people's lives in the region. This work comprehensively brought out the importance of this climate-water resources-agriculture-society connection.

Climate change will put additional pressure on producing regions such as Western Bahia. The projections intensify and increase the frequency of extreme precipitation and pluvial floods in NEB and a dominant increase in drought duration (IPCC, 2022). These changes can mainly shift the seasonality between the periods of drought and rain, increasing the dry period and consequently delaying the rainy season's onset. Therefore, adapting to these changes emphasize the need for planning and specific technologies for the region.

One of the solutions to adapt to these changes is the investment in monitoring. As mentioned in Chapter 1, the crucial element for a monitoring system is data: more groundwater monitoring wells; more telemetry stations, which make it possible to predict minimum discharge; real-time measurements of water used by irrigators. All this data should be centralized and processed in a situation room. Additional crucial investment is in highly skilled labor to design, operate and update such region-specific monitoring systems.

With improvement in water management strategies, there may come a time when the preservation of the environment should be treated as an investment and not a cost.

Future research efforts should focus on:

- climate projections for regional hydrology;

- the role of additional climate machanisms that can influence the rainfall regime in the region, such as the SACZ (South Atlantic Convergence Zone) or the SAMS (South America Monsson System);
- determination of Western Bahia's complex climate transition zone;
- obtaining a prediction model to forecast the December-January precipitation in Regions 1 and 2, using the lag correlations verified in Chapter 2.

References

ABAPA (2020). Produtores ruais defendem aumento da agricultura irrigada sustentável na Bahia. Available from: https://abapa.com.br/mais-noticias/produtores-rurais-defendem-aumento-da-agricultura-irrigada-sustentavel-na-bahia/.

AIBA. (2016). Anuário agropecuário Oeste da Bahia. Available from: http://aiba.org.br/wp-content/uploads/2017/03/Anuario-2015-16-FINAL-Web.pdf

AIBA (2017). Anuário Agropecuário Oeste da Bahia—Safra 2015/2016. Available from: http://aiba.org.br/wp-content/uploads/2018/06/anuario-16-17.pdf

AIBA. (2018). Aiba anuário safra 2017/2018. Available from: https://aiba.org.br/wp-content/uploads/2019/06/Anu%C3%A1rio-2019-Portugu%C3%AAs-Digital.pdf.

AIBA. (2020). RURAL Sustentabilidade. AIBA Rural - A Revista Do Agronegócio Da Bahia #17. Available from: https://aiba.org.br/wp-content/uploads/2020/09/AibaRural-Edicao-17-Digital.pdf

Alvares, C. A., Stape, J. L., Sentelhas, P. C., de Moraes Gonçalves, J. L., and Sparovek, G. (2014). Köppen's climate classification map for Brazil. *Meteorologische Zeitschrift*, *22*(6), 711–728. https://doi.org/10.1127/0941-2948/2013/0507

Almeida, W.A.; Moreira, M.C. (2014). Análise das outorgas da bacia do Rio Grande, Estado da Bahia. In Proceedings of the XLII Congresso Brasileiro de Engenharia Agrícola—CONBEA 2013, Campo Grande, Brazil, 27–31 July 2014.

Ambrizzi, T.; Souza, E.B.; Pulwarty, R.S. (2004). The Hadley and Walker Regional Circulations and Associated ENSO Impacts on the South American Seasonal Rainfall. In The Hadley Circulation: Present, Past and Future; Diaz, H.F., Bradley, R.S., Eds.; Kluwer Academic: Dordrecht, The Netherlands, 21, pp. 203–235. DOI: 10.1007/978-1-4020-2944-8_8

ANA (2013). Estudos hidrogeológicos na Bacia Hidrográfica do São Francisco—Sistema Aquífero Urucuia/Areado e Sistema Aquífero Bambuí. Comitê Bacia Hidrográfica do São Francisco. 2013. Available from: http://cbhsaofrancisco.org.br

ANA (2017). Atlas de Irrigação—Uso da Água na Agricultura. Available from: http://arquivos.ana.gov.br/imprensa/publicacoes/AtlasIrrigacao-UsodaAguanaAgriculturaIrrigada.pdf.

Araújo, M. L. S. de, Sano, E. E., Bolfe, É. L., Santos, J. R. N., dos Santos, J. S., & Silva, F. B. (2019). Spatiotemporal dynamics of soybean crop in the Matopiba region, Brazil (1990–2015). *Land Use Policy*, 80(September 2018), 57–67. https://doi.org/10.1016/j.landusepol.2018.09.040

Batistela, M.; Valladares, G.S., (2009) Farming expansion and land degradation in Western Bahia, Brazil. *Biota Neotrop.*, *9*, 61–76. https://doi.org/10.1590/S1676-06032009000300005

Bjerknes, J. (1969). Atmospheric Teleconnections From the Equatorial Pacific. *Monthly Weather Review*, *97*(3), 163–172. http://journals.ametsoc.org/doi/abs/10.1175/1520-0493(1969)097%3C0163:ATFTEP%3E2.3.CO;2

Bayazit, M. (2015). Nonstationary of hydrological records and recent trends in trend analysis: A state-of-the-art review. *Environ. Process.*, 2, 247–542. DOI 10.1007/s40710-015-0081-7

CBHRC (2015). Deliberação CBHRC 01/2015. Available from: https://www.conjur.com.br/dl/deliberacao-comite-bacia-corrente.pdf .

CGEE (2016) - CENTRO DE GESTÃO E ESTUDOS ESTRATÉGICOS. Desertificação, degradação da terra e secas no Brasil. Brasília, DF,. 252p. Available from: www.cgee.org.br

Correio 24 horas (2017). Guerra pela água em Correntina se arrasta desde 2015. Available from: https://www.correio24horas.com.br/noticia/nid/guerra-pela-agua-em-correntina-se-arrasta-desde-2015/

Cunha, Euclydes da, (1902): Os Sertões. Francisco Alves, Rio de Janeiro, 632p.

Delworth, T. L., and Mann, M. E. (2000). Observed and simulated multidecadal variability in the Northern Hemisphere. *Climate Dynamics*, *16*(9), 661–676. https://doi.org/10.1007/s003820000075

Dias, L. C. P., Pimenta, F. M., Santos, A. B., Costa, M. H., & Ladle, R. J. (2016). Patterns of land use, extensification, and intensification of Brazilian agriculture. *Global Change Biology*, 22(8), 2887–2903. https://doi.org/10.1111/gcb.13314

Dionizio, E. A., Pimenta, F. M., Lima, L. B., & Costa, M. H. (2020). Carbon stocks and dynamics of different land uses on the Cerrado agricultural frontier. *PLoS ONE*, 15(11 November), 1–22. https://doi.org/10.1371/journal.pone.0241637

Enfield, D. B., and Cid-Serrano, L. (2010). Secular and multidecadal warmings in the North Atlantic and their relationships with major hurricane activity. *International Journal of Climatology*, *30*(2), 174–184. https://doi.org/10.1002/joc.1881

Enfield, D. B., Mestas-Nuñez, A. M., and Trimble, P. J. (2001). The Atlantic Multidecadal Oscillation and its relation to rainfall and river flows in the continental U.S. *Geophysical Research Letters*, *28*(10), 2077–2080. https://doi.org/10.1029/2000GL012745

EMBRAPA (2020) Dinâmica Agrícola no Cerrado. ISBN 978-85-7035-951-3 v. 1.

Faleiro FG, de Farias neto AL. (2008). Savanas: desafios e estratégias para o equilı´brio entre sociedade, agronegócio e recursos naturais. Planaltina, DF: Embrapa Cerrados, Available from: https://www.alice.cnptia.embrapa.br/alice/handle/doc/570974

Folland, C. K., Palmer, T. N., and Parker, D. E. (1986). Sahel rainfall and worldwide sea temperatures, 1901-85. *Nature*, *320*(6063), 602–607. https://doi.org/10.1038/320602a0

Funk, C., Peterson, P., Landsfeld, M., Pedreros, D., Verdin, J., Shukla, S., Husak, G., Rowland, J., Harrison, L., Hoell, A., and Michaelsen, J. (2015). The climate hazards infrared precipitation with stations - A new environmental record for monitoring extremes. *Scientific Data*, *2*, 1–21. https://doi.org/10.1038/sdata.2015.66

G1 (2017). Grupo invade fazendas e incendeia galpão em protesto no Oeste da Bahia. Available from: https://g1.globo.com/bahia/noticia/grupo-invade-fazendas-e-incendeia-galpao-em-protesto-no-oeste-da-bahia.ghtml

Hastenrath, S., and Heller, L. (1977). Dynamics of climatic hazards in northeast Brazil. *Quarterly Journal of the Royal Meteorological Society*, *103*(435), 77–92. https://doi.org/10.1002/qj.49710343505

Hoff, H. (2011). Understanding the Nexus. Background Paper for the Bonn2011 Conference: The Water, Energy and Food Security Nexus. Stockholm Environment Institute, Stockholm.

IPCC, 2022: Summary for Policymakers [H.-O. Pörtner, D.C. Roberts, E.S. Poloczanska, K. Mintenbeck, M. Tignor, A. Alegría, M. Craig, S. Langsdorf, S. Löschke, V. Möller, A. Okem (eds.)]. In: Climate Change 2022: Impacts, Adaptation, and Vulnerability. Contribution of Working Group II to the Sixth Assessment Report of the Intergovernmental Panel on Climate Change [H.-O. Pörtner, D.C. Roberts, M. Tignor, E.S. Poloczanska, K. Mintenbeck, A. Alegría, M. Craig, S. Langsdorf, S. Löschke, V. Möller, A. Okem, B. Rama (eds.)]. Cambridge University Press. In Press.

Kane, R.P. (1997) Prediction of Droughts in North-East Brazil: Role of ENSO and Use of Periodicities. *Int. J. Climatol.*, 17, 655–665. DOI: 10.1002/(SICI)1097-0088(199705)17:6<655::AID-JOC144>3.0.CO;2-1

Kayano, M. T., Capistrano, V. B., Andreoli, R. V., and de Souza, R. A. F. (2016). A further analysis of the tropical Atlantic SST modes and their relations to north-eastern Brazil rainfall during different phases of Atlantic Multidecadal Oscillation. *International Journal of Climatology*, *36*(12), 4006–4018. https://doi.org/10.1002/joc.4610

Kayano, M. T., and Capistrano, V. B. (2014). How the Atlantic multidecadal oscillation (AMO) modifies the ENSO influence on the South American rainfall. *International Journal of Climatology*, *34*(1), 162–178. https://doi.org/10.1002/joc.3674

Kirtman, B.; Power, S.B.; Adedoyin, J.A.; Boer, G.J.; Bojariu, R.; Camilloni, I.; Doblas-Reyes, F.J.; Fiore, A.M.; Kimoto, M.; Meehl G.A.; et al. (2013). Near-term Climate Change: Projections and Predictability. In Climate Change 2013: The Physical Science Basis. Contribution of Working Group I to the Fifth Assessment Report of the Intergovernmental Panel on Climate Change; Stocker, T.F., Qin, D., Plattner, G.-K., Tignor, M., Allen, S.K., Boschung, J., Nauels, A., Xia, Y., Bex, V., Midgley P.M., Eds.; Cambridge University Press: Cambridge, UK; New York, NY, USA, pp. 953–1028.

Knight, J. R., Folland, C. K., and Scaife, A. A. (2006). Climate impacts of the Atlantic multidecadal oscillation. *Geophysical Research Letters*, *33*(17), 2–5. https://doi.org/10.1029/2006GL026242

Knudsen, M. F., Seidenkrantz, M. S., Jacobsen, B. H., and Kuijpers, A. (2011). Tracking the Atlantic Multidecadal Oscillation through the last 8,000 years. *Nature Communications*, *2*(1). https://doi.org/10.1038/ncomms1186

Landau, E.C.; Guimarães, D.P.; Souza, D.L. (2014). Concentração de áreas irrigadas por pivôs no Oeste da Bahia. In Anais do Simpósio Regional de Geoprocessamento e Sensoriamento Remoto; GEONORDESTE: Aracajú, Brazil, 18–21 November 2014. Available fom: https://ainfo.cnptia.embrapa.br/digital/bitstream/item/119284/1/Concentracao-areas.pdf

Li, Z., Zhang, W., Jin, F.-F., Stuecker, M. F., Sun, C., Levine, A. F. Z., Xu, H., and Liu, C. (2020). A robust relationship between multidecadal global warming rate variations and the Atlantic Multidecadal Variability. *Climate Dynamics*, *55*(7–8), 1945–1959. https://doi.org/10.1007/s00382-020-05362-8

Liu, G., and Kwon, Y. (2021). Predicting Atlantic Multidecadal Variability. *Workshop at NeurIPS 2021*, 1–7.

Magrin, G.O.; Marengo, J.A.; Boulanger, J.-P.; Buckeridge, M.S.; Castellanos, E.; Poveda, G.; Scarano, F.R.; Vicuña, S. (2014). Central and South America. In Climate Change 2014: Impacts, Adaptation, and Vulnerability. Part B: Regional Aspects. Contribution of Working Group II to the Fifth Assessment Report of the Intergovernmental Panel on Climate Change; Barros, V.R., Field, C.B., Dokken, D.J., Mastrandrea, M.D., Mach, K.J., Bilir, T.E., Chatterjee, M., Ebi, K.L., Estrada, Y.O., Genova, R.C., et al., Eds.; Cambridge University Press: Cambridge, UK; New York, NY, USA, pp. 1499–1566.

Mann, M. E., Steinman, B. A., and Miller, S. K. (2014). On forced temperature changes, internal variability, and the AMO. *Geophysical Research Letters*, *41*(9), 3211–3219. https://doi.org/10.1002/2014GL059233

Marengo, J. A., Torres, R. R., and Alves, L. M. (2017). Drought in Northeast Brazil—past, present, and future. *Theoretical and Applied Climatology*, *129*(3–4), 1189–1200. https://doi.org/10.1007/s00704-016-1840-8

Marques, E. A. G., Silva Junior, G. C., Eger, G. Z. S., Ilambwetsi, A. M., Raphael, P., Generoso, T. N., Oliveira, J., and Júnior, J. N. (2020). Analysis of groundwater and river stage fluctuations and their relationship with water use and climate variation effects on Alto Grande watershed, Northeastern Brazil. *Journal of South American Earth Sciences*, *103*, 102723. https://doi.org/10.1016/j.jsames.2020.102723

Massey Jr., F.J. (1951) The Kolmogorov-Smirnov Test for Goodness of Fit. *Journal of the American Statistical Association*, 46, 68-78. https://doi.org/10.1080/01621459.1951.10500769

McCarthy, G. D., Haigh, I. D., Hirschi, J. J. M., Grist, J. P., and Smeed, D. A. (2015). Ocean impact on decadal Atlantic climate variability revealed by sea-level observations. *Nature*, *521*(7553), 508–510. https://doi.org/10.1038/nature14491

MDIC (2017) - Ministério do Desenvolvimento, Indústria e Comércio Exterior. Panorama Agroeconômico do Oeste da Bahia e Safra 2016/17. Available from: http://www.mdic.gov.br/images/REPOSITORIO/czpe/Eventos/ZPE_Agroneg%C3%B3cio/Panorama_do_agroneg%C3%B3cio_baiano_Aiba__Celestino_Zanella.pdf

Mitchell, J.M., Jr.; Dzerdzeevskii, B.; Flohn, H.; Hofmeyr, W.L.; Lamb, H.H.; Rao, K.N.; Wallén, C.C. (1966) Climatic Change; WMO Technical Note No. 79; World Meteorological Organization: Geneva, Switzerland.

MME (2019). Ministério de Minas e Energia. Empresa de Pesquisa Energética, Brazilian Energy Balance. Available from: http://epe.gov.br/en/publications/publications/brazilian-energy-balance

Moura, A. D., and Shukla, J. (1981). On the Dynamics of Droughts in Northeast Brazil: Observations, Theory and Numerical Experiments with a General Circulation Model. *Journal of the Atmospheric Sciences*, *38*(12), 2653–2675. https://doi.org/10.1175/1520-0469(1981)038<2653:OTDODI>2.0.CO;2

Oliveira, J.R.S.; Ribeiro, R.B.; Sousa, J.R.C.; Serrano, L.O.; Ramos, M.C.A.R.; Generoso, T.N.; Pruski, F.F. (2019). Hydrological Information System to quantify water availability (SIHBA). Unpublished.

Pettitt A.N. (1979). A non-parametric approach to the change-point problem. *Appl. Statist.*, 2, 126–135. https://doi.org/10.2307/2346729

Pousa, R., Costa, M. H., Pimenta, F. M., Fontes, V. C., and Castro, M. (2019). Climate change and intense irrigation growth in Western Bahia, Brazil: The urgent need for hydroclimatic monitoring. *Water (Switzerland)*, *11*(5). https://doi.org/10.3390/w11050933

Pruski, F.F.; Rodriguez, R.D.G.; Nunes, A.A.; Pruski, P.L.; Singh, V.P. (2015). Low-flow estimates in regions of extrapolation of the regionalization equations: a new concept. *Eng. Agrícola*, 35, 808–816. https://doi.org/10.1590/1809-4430-Eng.Agric.v35n5p808-816/2015

Richards, P.; Pellegrina, H.; VanWey, L.; Spera, S. (2015). Soybean development: The impact of a decade of agricultural change on urban and economic growth in Mato Grosso, Brazil. PLoS One, 10, e0122510. https://doi.org/10.1371/journal.pone.0122510

Rogers, P.; Hall, A.W. (2003). Effective Water Governance; Global Water Partnership Technical Committee Background Papers No. 7; Global Water Partnership: Stockholm, Sweden.

Rybski, D.; Bunde, A.; Havlin, S.; von Stoch, H. (2006). Long-term persistence in climate and the detection problem. *Geophys. Res. Lett.*, 33, 1–4. https://doi.org/10.1029/2005GL025591

Sampaio Ferraz, J. de, (1925). *Causas provaveis das secas do Nordeste Brasileiro*. Ministerio de Agricultura, Directoria de Meteorologia, Rio de Janeiro, 12 pp.

Sampaio Ferraz, J. de, (1950): Iminência de uma grande seca no Nordeste. Rev. Bras. Geografia, 12, 3-15p.

Santos, A. B., Costa, M. H., Mantovani, E. C., Boninsenha, I., and Castro, M. (2020). A remote sensing diagnosis of water use and water stress in a region with intense irrigation growth in brazil. *Remote Sensing*, *12*(22), 1–16. https://doi.org/10.3390/rs12223725

Serinaldi, F.; Kilsby, C.G. (2005). Stationarity is undead: Uncertainty dominates the distribution of extremes. *Adv. Wat. Res.*, 77, 17–36. https://doi.org/10.1016/j.advwatres.2014.12.013

Shimizu, M. H., Anochi, J. A., and Kayano, M. T. (2021). Precipitation patterns over northern Brazil basins: climatology, trends, and associated mechanisms. *Theoretical and Applied Climatology*, *147*(1–2), 767–783. https://doi.org/10.1007/s00704-021-03841-4

Silva, A. L. da, Souza, S. A. de, Coelho Filho, O., Eloy, L., Salmona, Y. B., and Passos, C. J. S. (2021). Water appropriation on the agricultural frontier in western Bahia and its contribution to streamflow reduction: Revisiting the debate in the Brazilian cerrado. *Water (Switzerland)*, *13*(8). https://doi.org/10.3390/w13081054

Soterroni, A. C., Ramos, F. M., Mosnier, A., Fargione, J., Andrade, P. R., Baumgarten, L., Pirker, J., Obersteiner, M., Kraxner, F., Câmara, G., Carvalho, A. X. Y., & Polasky, S. (2019). Expanding the Soy Moratorium to Brazil's Cerrado. *Science Advances*, *5*(7). https://doi.org/10.1126/sciadv.aav7336

Ting, M., Kushnir, Y., Seager, R., and Li, C. (2009). Forced and internal twentieth-century SST trends in the North Atlantic. *Journal of Climate*, *22*(6), 1469–1481. https://doi.org/10.1175/2008JCLI2561.1

Trewartha GT. (1961). *The Earth's problem climates*. University of Wisconsin Press, Madison, p 371.

UNESCO (2006). United Nations Educational, Scientific and Cultural Organization; World Water Assessment Programme. Water, a Shared Responsibility; The United Nations World Water Report 2; Berghahn Books: Paris, France; New York, NY, USA, pp. 43–86.

Vieira, M. de S. B., Campos, J. E. G., Pinto, J. de A., and Santos, M. S. (2021). The Relationship Between The Atlantic Multidecadal Oscillation and The Urucuia Aquifer System Recharge. *Climate Dynamics*, 1–31. https://doi.org/doi.org/10.21203/rs.3.rs-806881/v1

Verdin, K.L.; Verdin, J.P. (1999). A topological system for delineation and codification of the Earth's river basins. J. Hydrol., 218, 1–12. https://doi.org/10.1016/S0022-1694(99)00011-6

Verstraeten, G.; Poesen, J.; Demarée, G.; Salles, C. (2006). Long-term (105 years) variability in rain erosivity as derived from 10-min rainfall depth data for Ukkel (Brussels, Belgium): Implications for assessing soil erosion rates. *J. Geophys. Res.* , 111, 1–11. https://doi.org/10.1029/2006JD007169

Xavier, A.C.; King, C.W.; Scanlon, B.R. (2015). Daily gridded meteorological variables in Brazil (1980–2013). Int. J. Climatol. 2016, 36, 2644–2659. https://doi.org/10.1002/joc.4518

Walker. (1928). "World Weather III,." *Memoirs of the Royal Meteorological Society*, *II*, 97-106.

Wang, C., and Zhang, L. (2013). Multidecadal ocean temperature and salinity variability in the tropical north atlantic: Linking with the AMO, AMOC, and subtropical cell. *Journal of Climate*, *26*(16), 6137–6162. https://doi.org/10.1175/JCLI-D-12-00721.1

WMEPE (2019)- Web Map EPE—Sistema de Informações Geográficas do Setor Energético Brasileiro. Available from: https://gisepeprd.epe.gov.br/webmapepe/#

Yang, X., Delworth, T. L., Zeng, F., Zhang, L., Cooke, W. F., Harrison, M. J., Rosati, A., Underwood, S., Compo, G. P., and McColl, C. (2021). On the Development of GFDL's Decadal Prediction System: Initialization Approaches and Retrospective Forecast Assessment. *Journal of Advances in Modeling Earth Systems*, *13*(11), 1–30. https://doi.org/10.1029/2021MS002529

Yoffe, S.; Fiske, G.; Giordano, M.; Giordano, M.; Larson, K.; Stahl, K.; Wolf, T. (2004) Geography of international water conflict and cooperation: Data sets and applications. *Water Resour. Res.*, 40, 1–12. https://doi.org/10.1029/2003WR002530